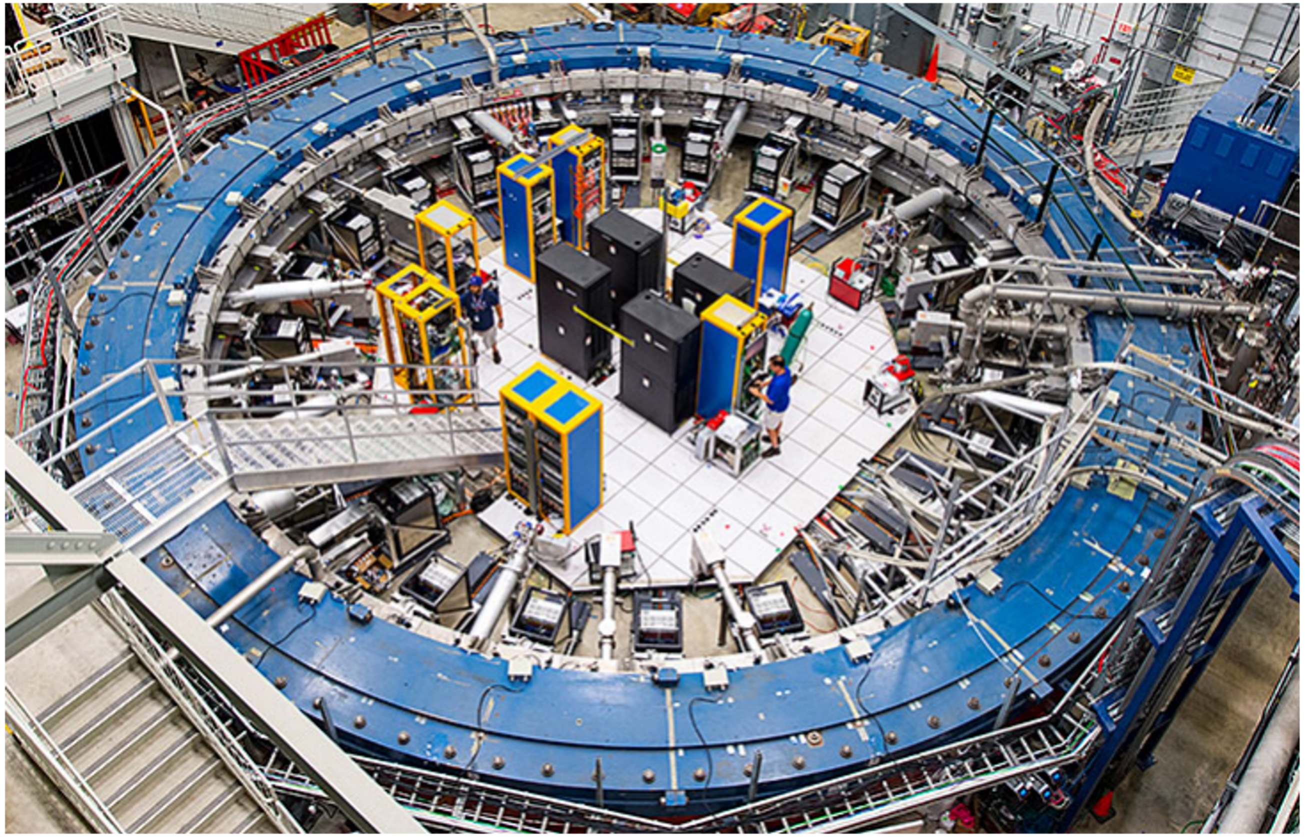

Beam Dynamics in the Muon g-2 Experiment at Fermilab

David A. Tarazona

23 March 2022

Outline

- a_μ Overview
- The Muon g-2 Storage Ring Magnet
- Muon beam
- Optical lattice
- Nonlinearities
- Beam dynamics systematic effects
- Summary, current status and plans

a_μ Overview: Run-1 Results

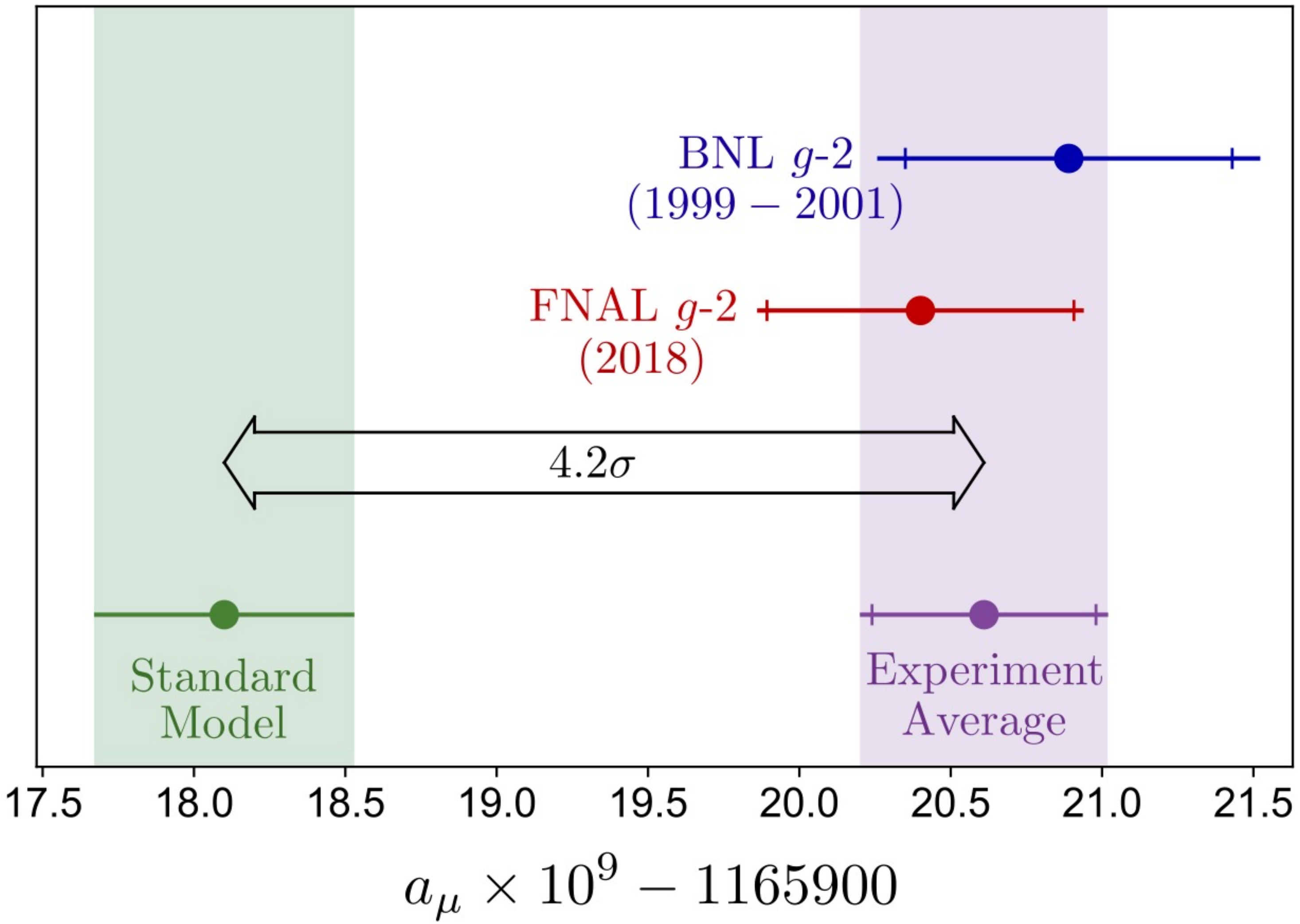

$$a_\mu(\text{FNAL}) = 116\,592\,040(54) \times 10^{-11} \quad (0.46\,\text{ppm})$$

$$a_\mu(\text{Exp}) = 116\,592\,061(41) \times 10^{-11} \quad (0.35\,\text{ppm})$$

- 3.3σ significance between SM and the latest experimental result.
- Confirmed the BNL result (0.6σ).
- Combined experimental average at 4.2σ tension with SM from theory initiative.
- Statistical uncertainties dominate the experimental average result.
- Run-1 data is only 6% of the target statistics… More to come.

$$a_\mu^{Exp} - a_\mu^{SM} = (251 \pm 59) \times 10^{-11}$$

a_μ Overview: a_μ from SM

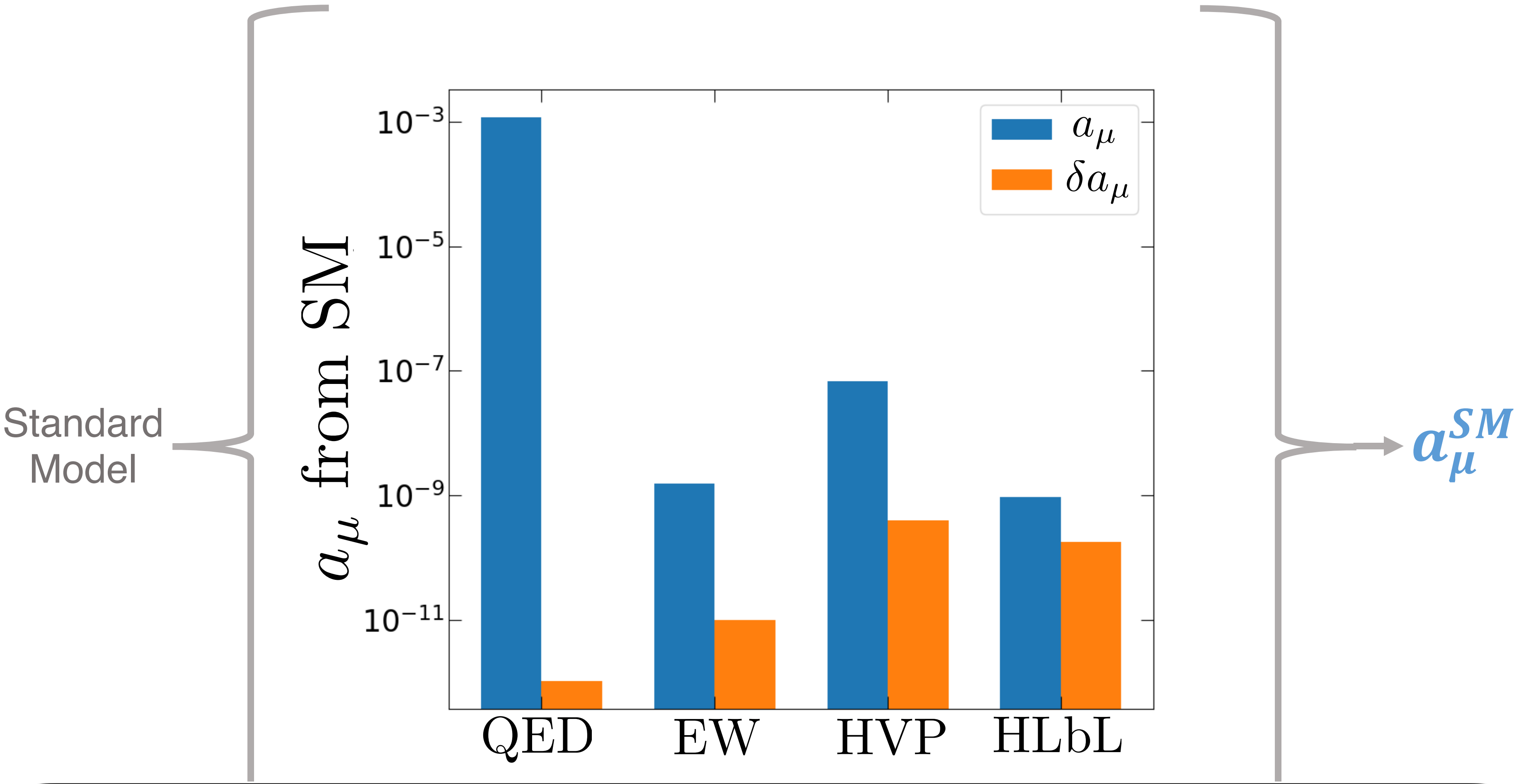

$$a_\mu^{\mathrm{SM}} = a_\mu^{\mathrm{QED}} + a_\mu^{\mathrm{Weak}} + a_\mu^{\mathrm{HVP}} + a_\mu^{\mathrm{HLbL}} = 116591810\,(43) \times 10^{-11}$$

*From Muon g-2 Theory Initiative: Phys. Rep. **887**, 1 (2020).

a_μ Overview: Experimental technique

- 1956: Lee and Yang → Parity violation in weak decays would provide a way to measure the muon magnetic moment.

In Rest Frame:
($\boldsymbol{s}$: spin, $\boldsymbol{p}$: momentum)

Pion decay
$\pi^+ \rightarrow \mu^+\nu_\mu$

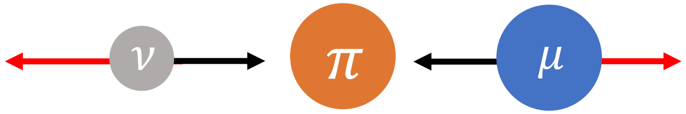

Muon decay
$\mu^+ \rightarrow e^+\nu_e\bar{\nu}_\mu$

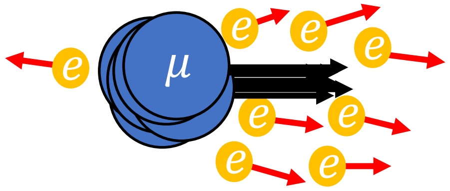

e : Higher-energy positrons

- In lab frame forward/backward muons from pion decay still highly polarized.

- From the parity-violating muon decay $\mu^+ \rightarrow e^+\nu_e\bar{\nu}_\mu$, highest energy positrons are emitted in the muon spin direction with a probability proportional to the angle between these two directions.

*Assume π's, μ's, and e's are positively charged, unless indicated otherwise.

Purpose of the Muon *g-2* Storage Ring

- Purpose: To provide ~3GeV positrons out of muon beam decay for calorimetry.

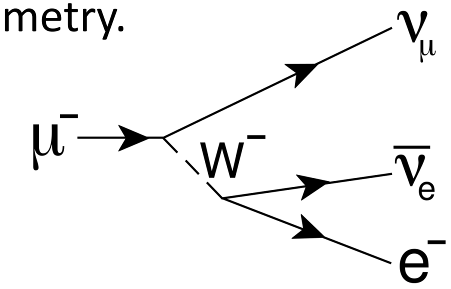

$$\omega_a = \omega_S - \omega_C = -\frac{e}{m_\mu} a_\mu \tilde{B}$$

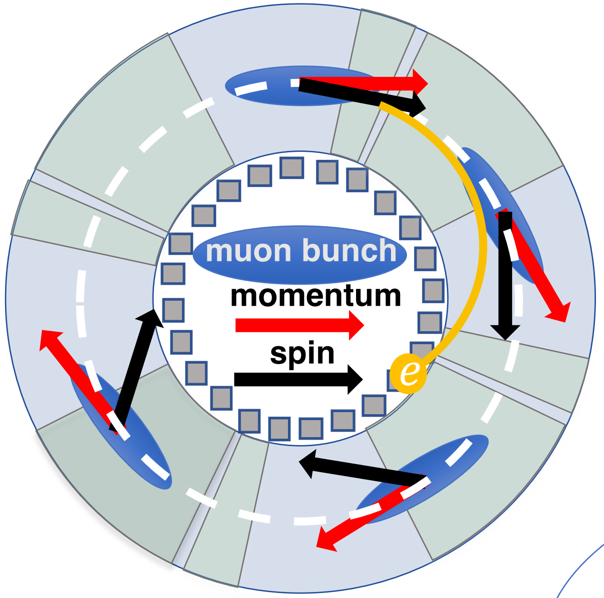

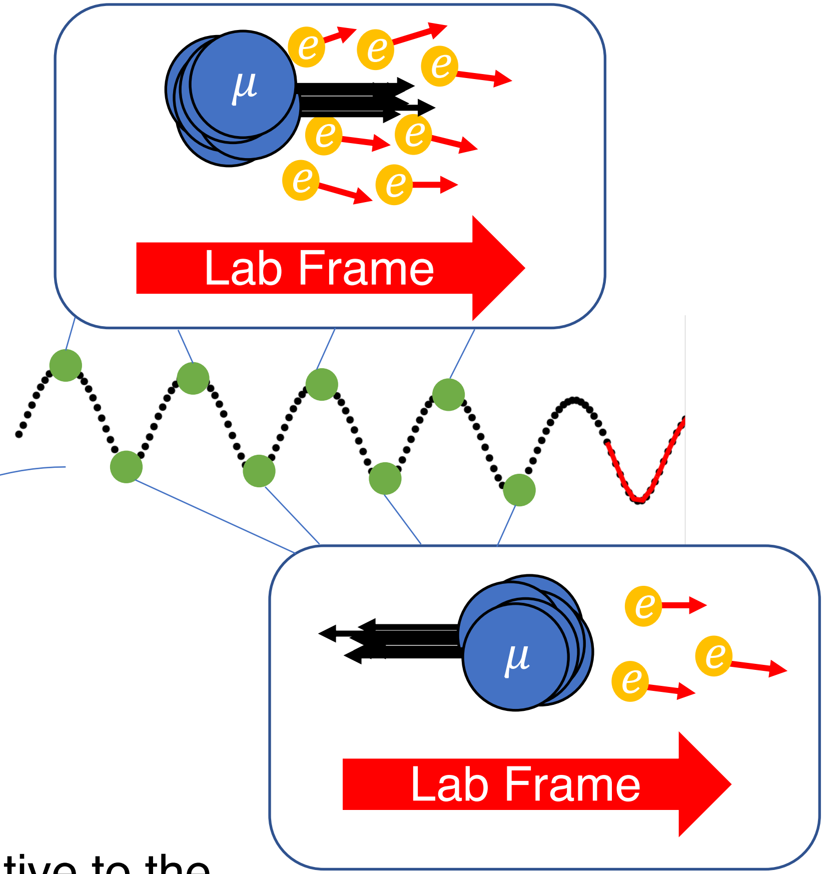

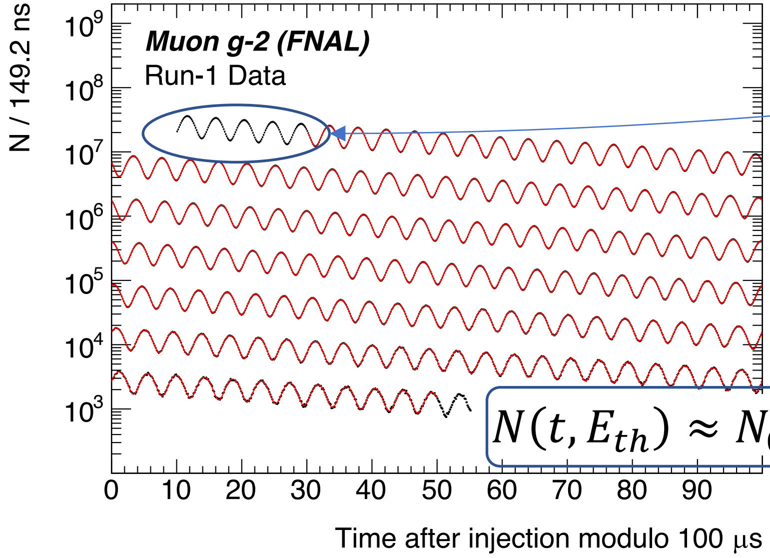

ω_a: Spin precession frequency relative to the momentum direction of muons in the of the storage ring

e: Higher-energy positrons

$$N(t, E_{th}) \approx N_0(E_{th}) \exp^{-t/\gamma\tau_\mu}[1 + A(E_{th}) \cos(\omega_a t + \varphi_0(E_{th}))]$$

Purpose of the Muon *g-2* Storage Ring

- The ring is designed to allow a highly precise measurement of the muon anomalous magnetic moment anomaly $a_\mu \equiv (g_\mu - 2)/2$ ($\Delta a_\mu / a_\mu \leq 140$ ppb):

$$a_\mu = \frac{\omega_a}{\tilde{\omega}'_p(T_r)} \frac{\mu'_p(T_r)}{\mu_e(H)} \frac{\mu_e(H)}{\mu_e} \frac{m_\mu}{m_e} \frac{g_e}{2}$$

Main measurements:

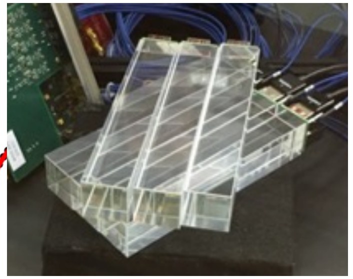

- ω_a: The "anomalous precession frequency"

- $\tilde{\omega}'_p$: Proton Larmor frequency measured in a spherical water sample, weighted by the muon distribution $\left(B = \frac{\hbar\omega_p}{2\mu_p}\right)$.

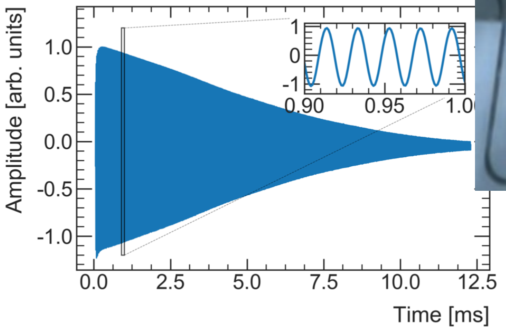

Ring parameters

Ring Parameter	Value*
Nominal momentum	3.094 GeV/c
Momentum acceptance	±0.56%
Horizontal tune	0.944
Vertical tune	0.330
Bending magnetic field	1.4512991 T
Bending radius	7.112 m
Revolution period	149.2 ns
β_x	[7.4,7.7] m
β_y	[21,22] m
D_x	[7.9,8.1] m
Horizontal admittance	268 π mm.mrad
Vertical admittance	93 π mm.mrad
Maximum excursion	45 mm
x' max	6 mrad
y' max	2 mrad
Focusing plates voltage	~18.3 kV
Vacuum in storage volume	≲1.5E-6 Torr
Current	5170 A

*Representative values

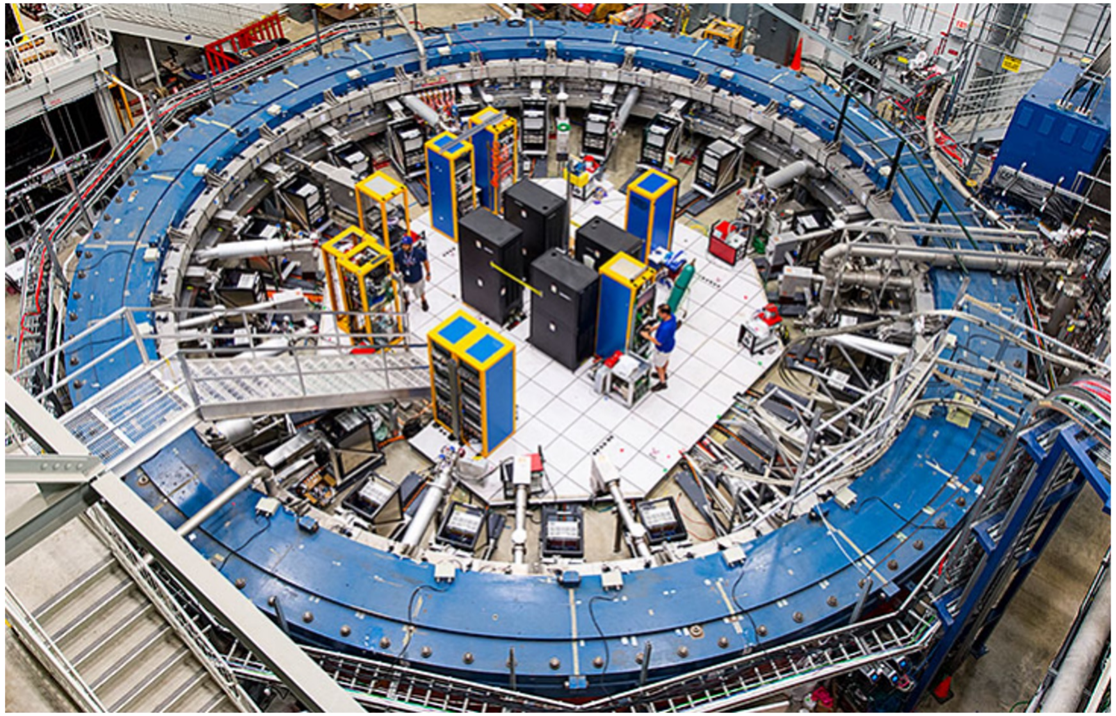

- Temporal stability and spatial homogeneity of the magnetic guide field are essential to the experiment.

- Average magnetic field experienced by stored muons needs to remain stable on the scale of ppm.

Main magnet

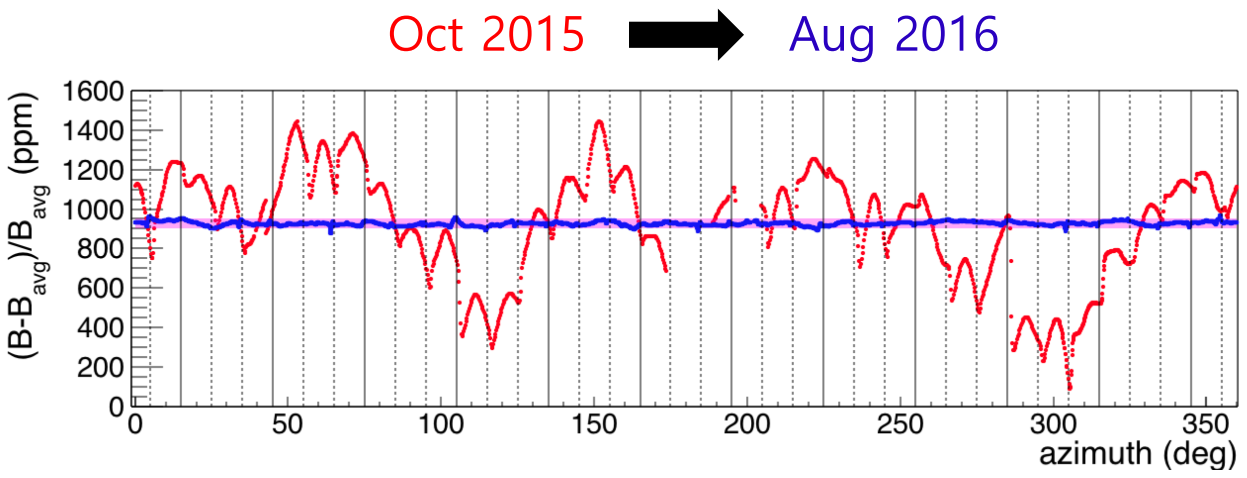

- Magnet shimming keeps the field highly uniform (local variations <50 ppm).

  - Passive shimming:
    - *Pole pieces positioning* drives the overall field strength.
    - *Additional pieces of iron* fine-tune azimuthally averaged field and control transverse gradients.

  - Active shimming:
    - *Surface coils* target specific azimuthally averaged multipole gradients.
    - *Power supply feedback* adjusts supply current to keep the average vertical field constant over time.

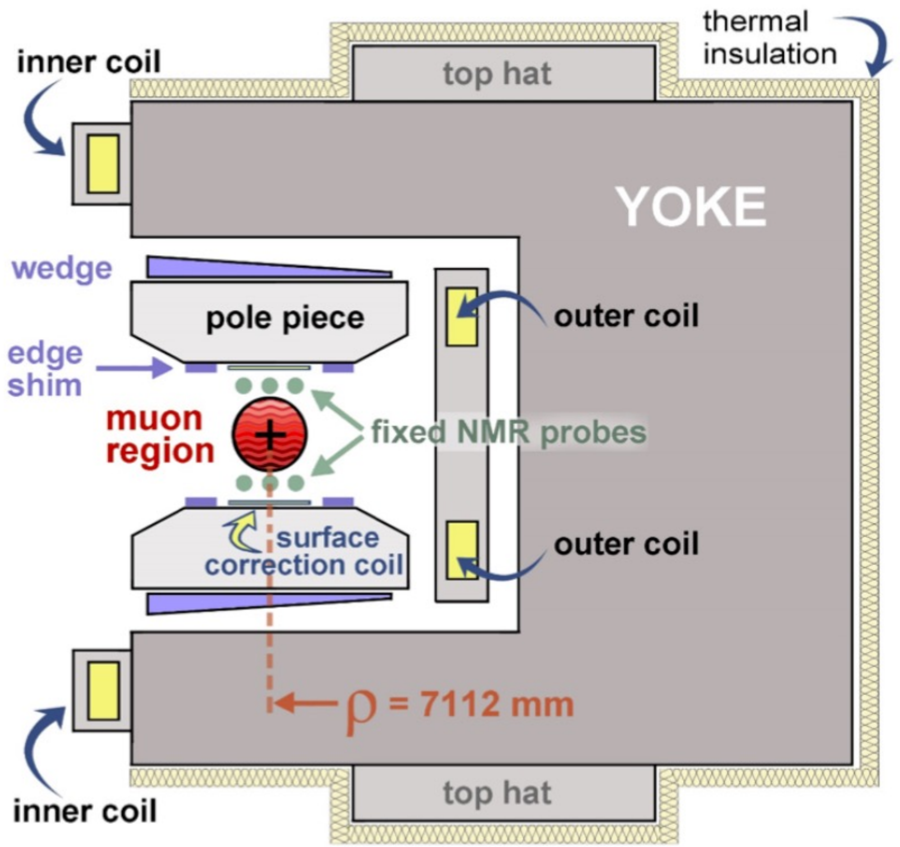

Magnetic field measurement (i.e., $\tilde{\omega}'_p$)

$$\tilde{B} = \frac{\hbar\tilde{\omega}'_p(T)}{2\mu'_p(T)} = \frac{\hbar\tilde{\omega}'_p(T)}{2}\frac{\mu_e(H)}{\mu'_p(T)}\frac{\mu_e}{\mu_e(H)}\frac{1}{\mu_e}$$

Known to ~10 ppb precision

$$\tilde{\omega}'_p(T_r) = f_{\text{calib}}\,\langle\omega_p(x,y,\phi)\times M(x,y,\phi)\rangle\,(1+B_k+B_q)$$

- f_{calib}: NMR probe calibration factor
- $\omega_p(x,y,\phi)$: Larmor frequency from proton NMR
- $M(x,y,\phi)$: Muon beam distribution
- B_k: Correction from beam injection system
- B_q: Correction from beam focusing system

Magnetic field measurement

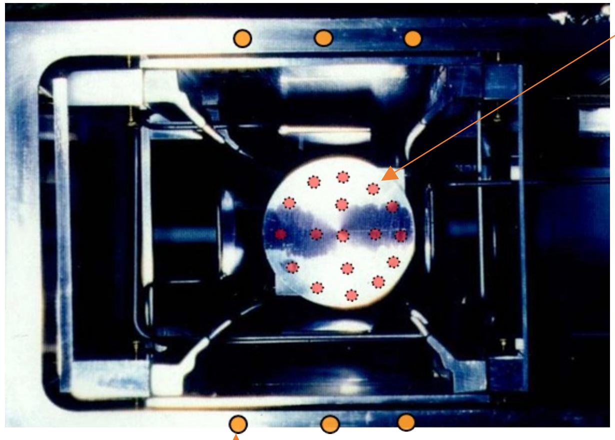

Field in storage region mapped out by NMR trolley every ~3 days.

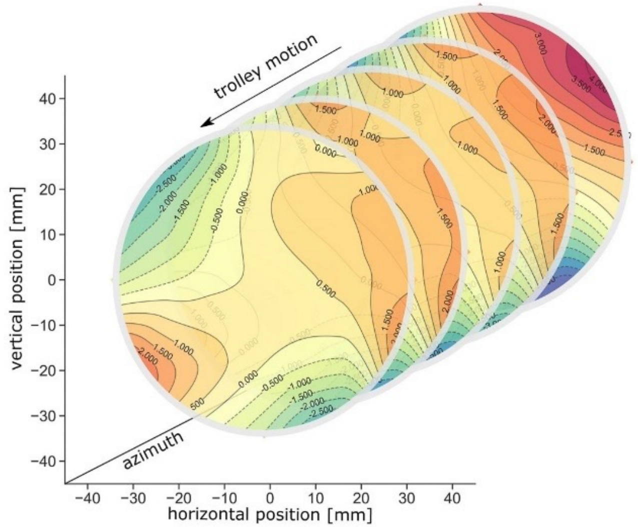

Field tracking between trolley runs is continuously tracked by 378 fixed NMR probes located throughout the ring.

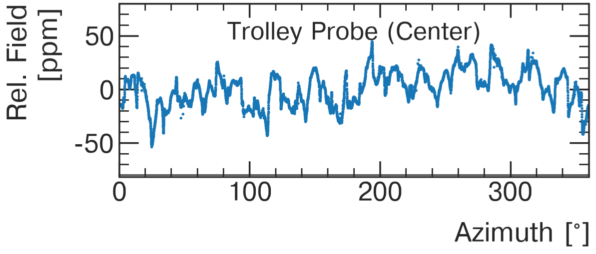

- Systematic effects associated with field mapping:
  - Position uncertainties (~5-25 ppb*)
  - Motion effects (~5-25 ppb)
  - Temperature effects (~5-25 ppb)
  - Configurations (<22 ppb)

- Systematic effects associated with field tracking, from tracking offsets for all fixed probe stations (~20-40 ppb).

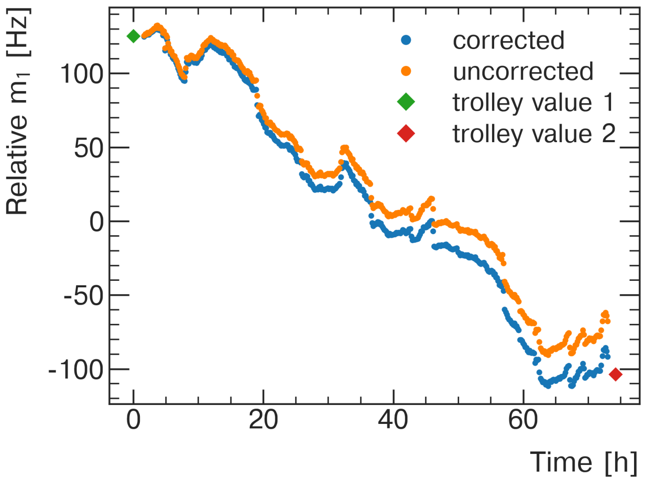

*Systematic errors representative of Run-1.

Magnetic field, beam-weighted

- 2D mapping of the field is described as a multipole expansion:

$$B \approx B_y = A_0 + \sum_{n=1}^{4} \left(\frac{r}{r_0}\right)^n \left(A_n \cos(n\theta) + B_n \sin(n\theta)\right)$$

- Local variations of radial and azimuthal fields (typically <100 ppm of main field) lead to $(B - B_y)/B = O(10\text{ ppb})$.

- The weighting simplifies to combining normal/skew terms in field expansion (c_n, s_n) with beam's multipole normal/skew projections (I_n, J_n) along azimuth:

$$\tilde{B} = c_0 + \sum_{n=1}^{4} (c_n I_n + s_n J_n)$$

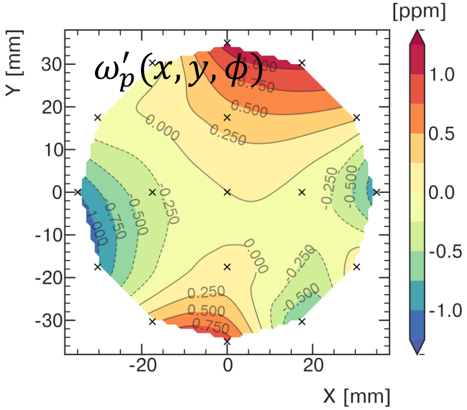

x

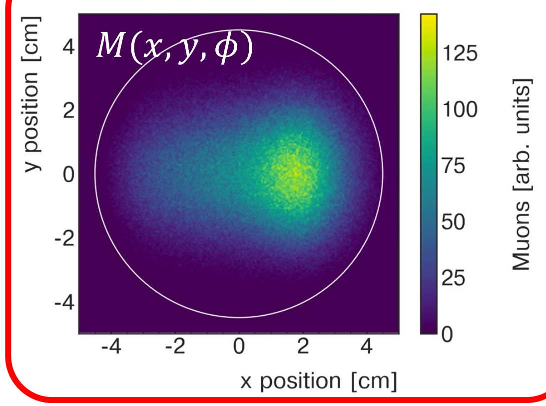

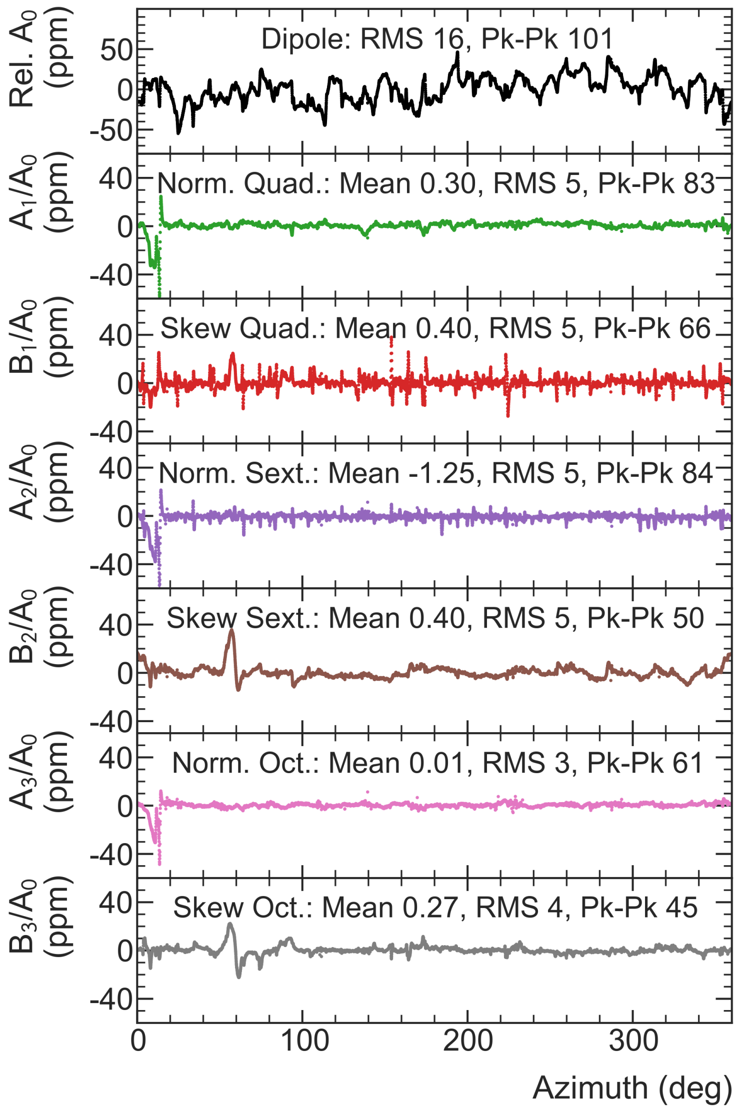

Muon beam production

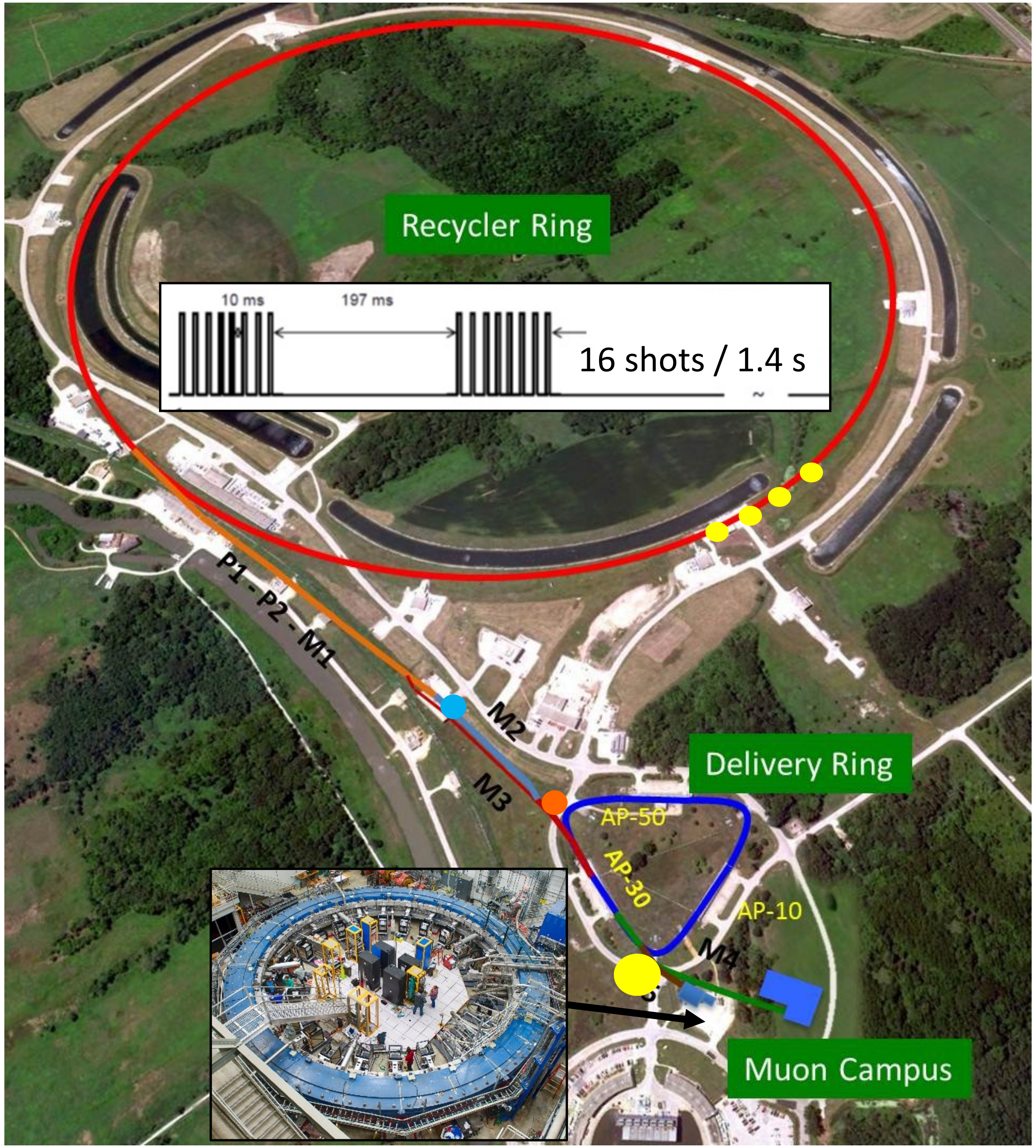

- 10^{12} protons per pulse (~ 8.89GeV) hit the production target.
- From parity violation in $\pi^+ \to \mu^+ \nu_\mu$ decays, muons are highly polarized.
- Fermilab's Muon Campus beamlines transport ~3.1 GeV/c muons to storage ring.
- Muon beam is purified in Delivery Ring.

Muon beam injection

- **Injection** kickers aim to align muons with storage region.

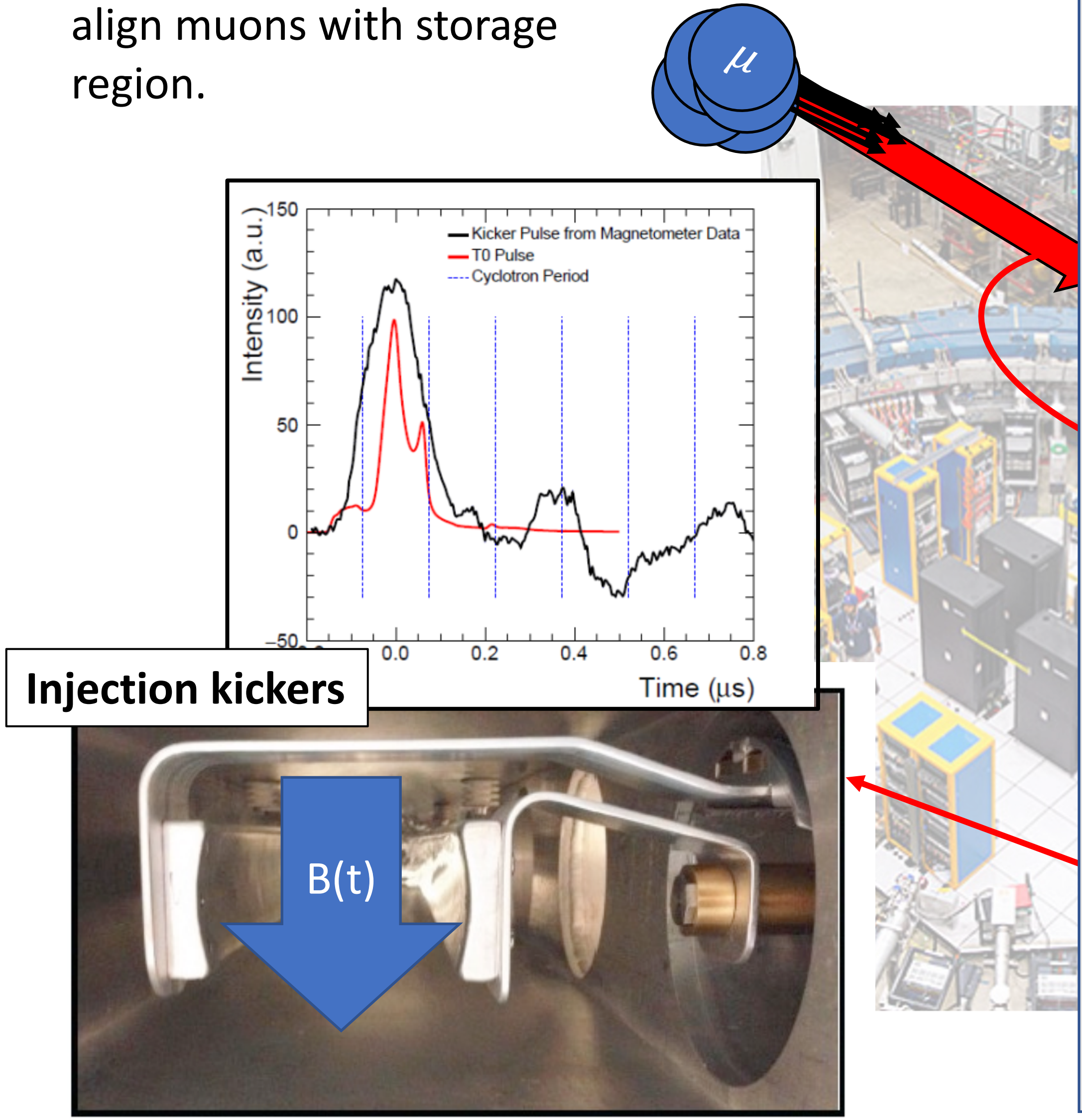

Kicker transient field

- Fast kicker pulses impedance mismatch induces eddy currents.
- Faraday magnetometer using fibers measured the kicker transient field (laser polarization rotates in TGG crystal in presence of the magnetic field).

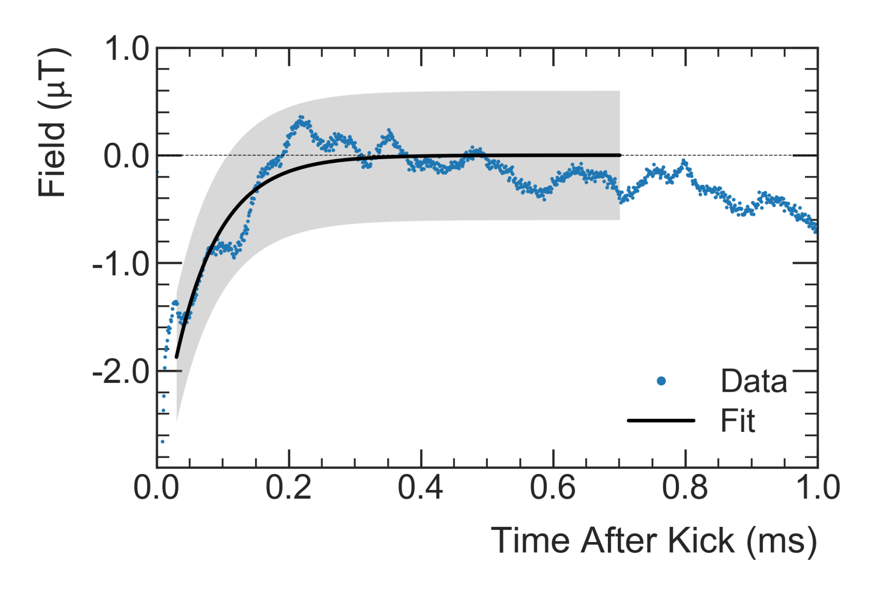

$B_k = -27(37)$ ppb for Run-1

Muon beam injection

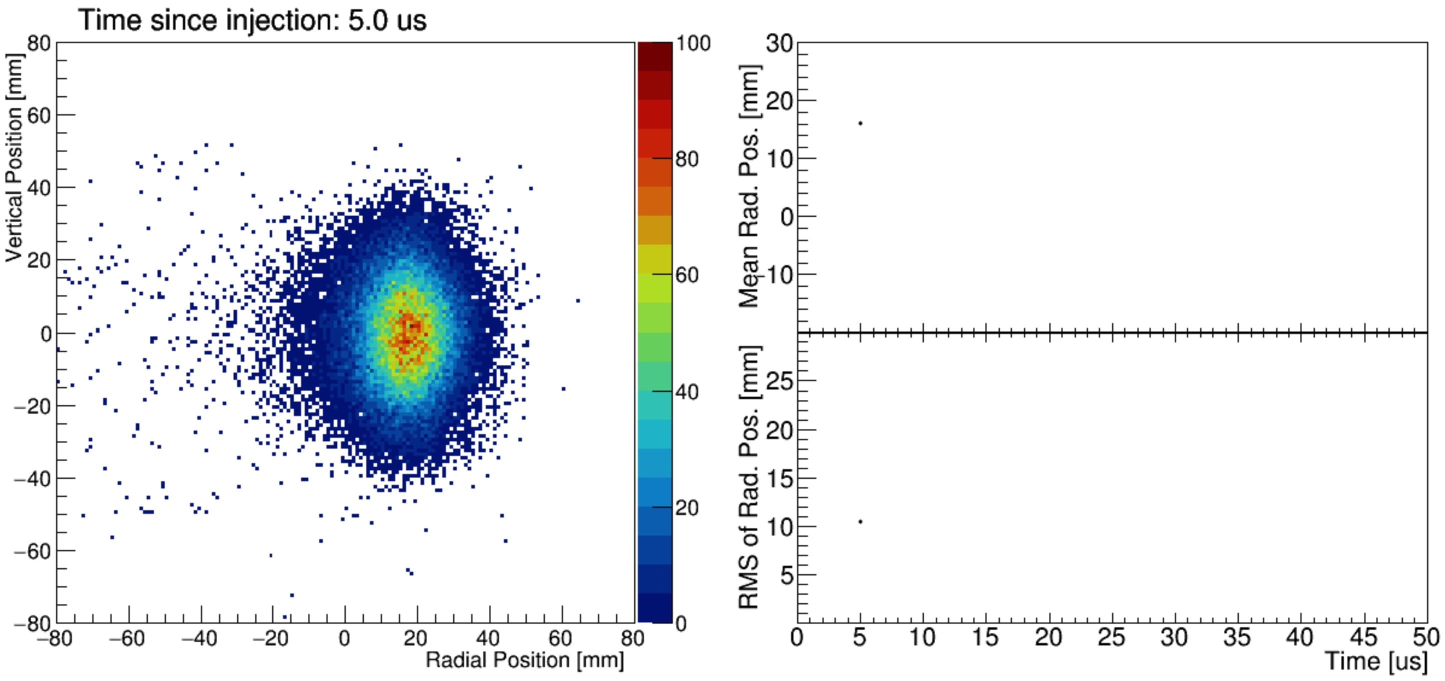

- Imperfect injection kick creates beam's radial centroid oscillation (aka "Coherent Betatron Oscillation" CBO).

$$f_{CBO} = f_C(1 - Q_x) \approx 0.37 \text{ MHz}$$

- Optics mismatch between injected beam and ring produces beam's radial width oscillation.

- Beam's transverse profile is measured with gaseous straw tracking detector:

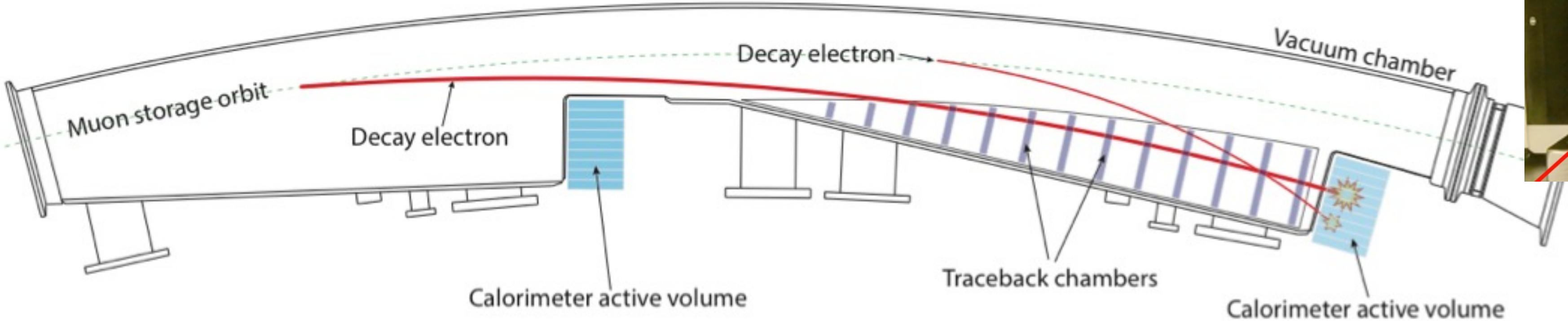

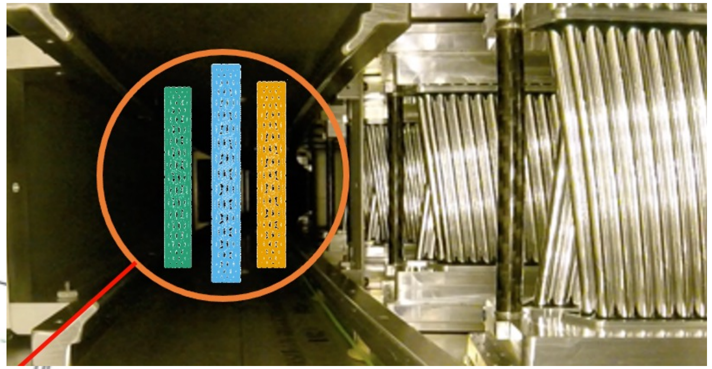

Muon beam vertical confinement

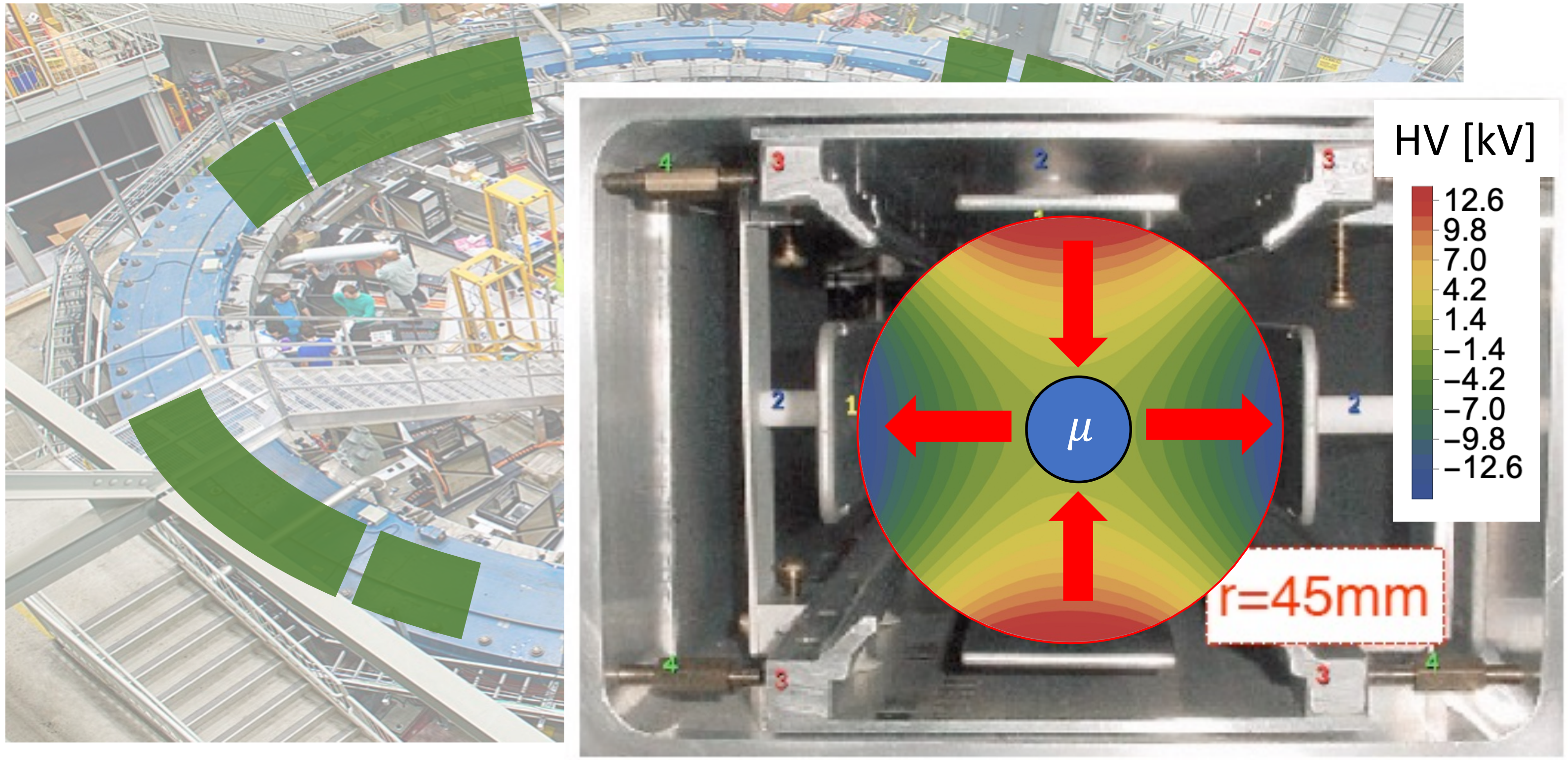

Quad plates mechanical vibration

- The ESQ plates are pulsed at 100 Hz.
- Mechanical vibrations induce a magnetic field transient in the storage region.

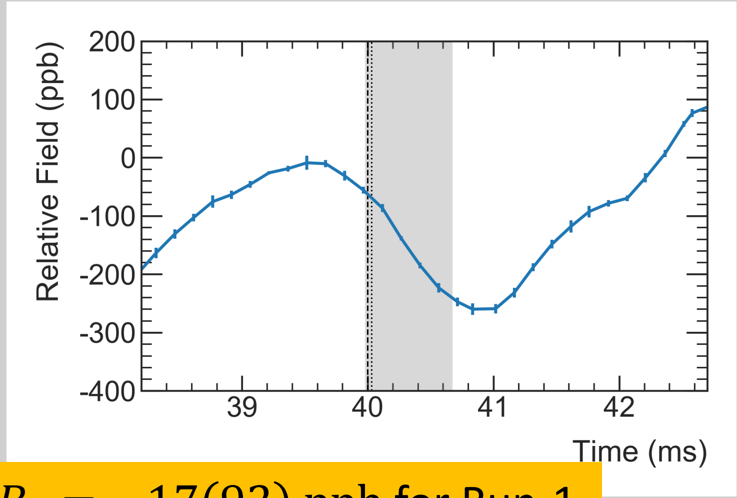

$B_q = -17(92)$ ppb for Run-1

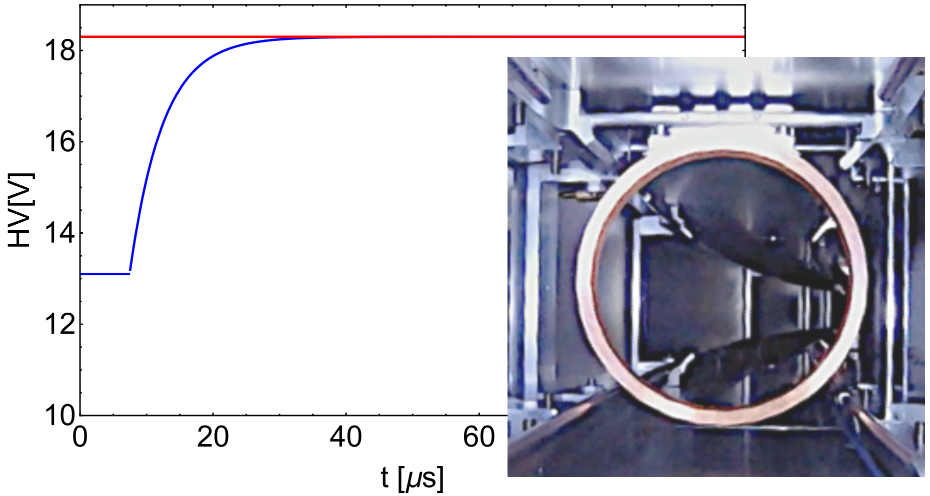

- The ElectroStatic Quadrupole system (ESQ) provides vertical focusing.
- The ESQ plates are mis-powered for closed orbit distortions.

Optical lattice

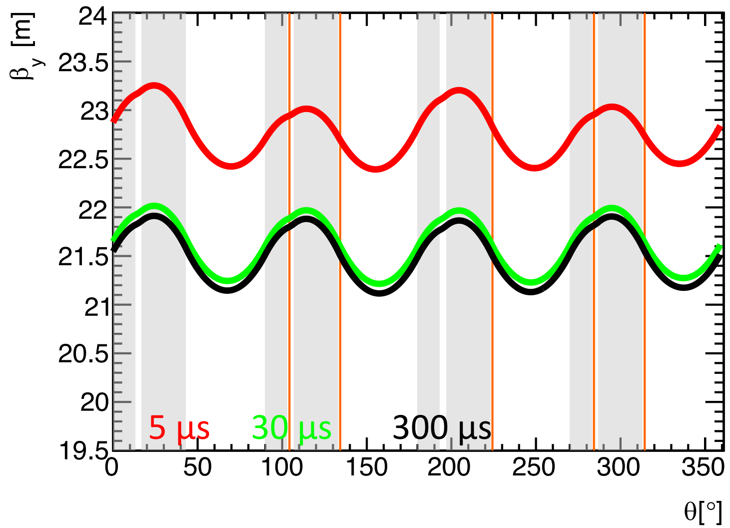

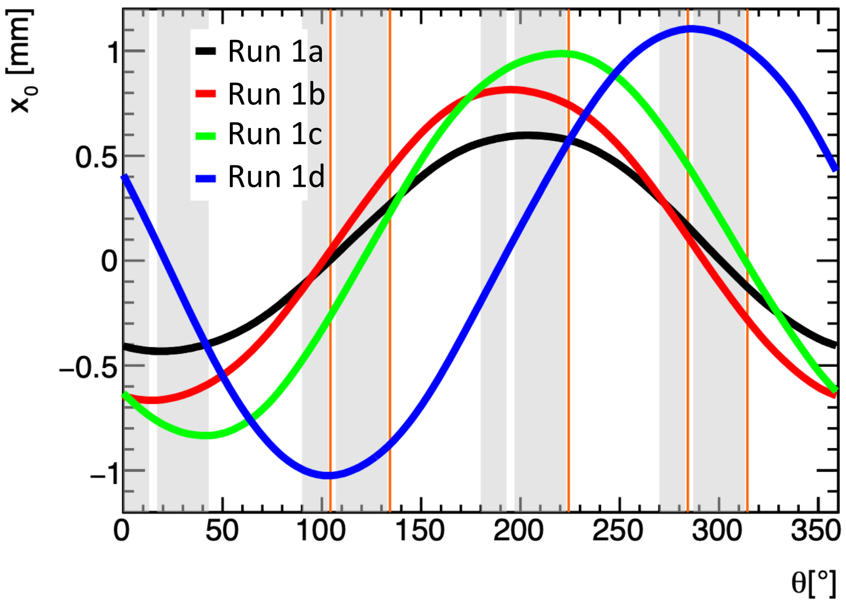

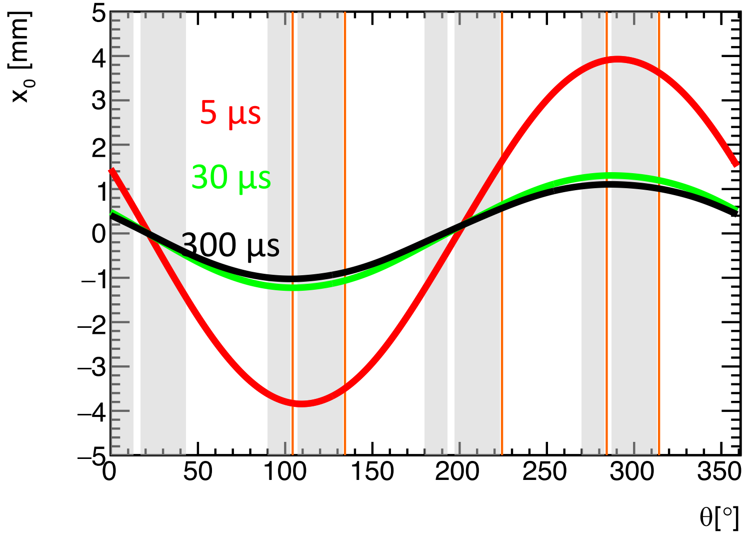

- Beam stability is provided by relatively weak focusing:

$$x'' + \frac{1-n}{\rho_0^2}x = 0$$
$$y'' + \frac{n}{\rho_0^2}y = 0$$

- Field index n from ESQ system:

$$n = \frac{\rho_0}{vB_0}\frac{\partial E_y}{\partial y}$$

$$n \approx 0.1 \quad , \quad 0 \leq n \leq 1$$

- Weak-focusing modelling provides 1st order ring representation:

$$\beta_x(s) \approx \frac{\rho_0}{\sqrt{1-n}} \qquad \beta_y(s) \approx \frac{\rho_0}{\sqrt{n}} \qquad D_x(s) \approx \frac{\rho_0}{1-n}$$

$$Q_y \approx \sqrt{n} \qquad Q_x \approx \sqrt{1-n}$$

Nonlinearities

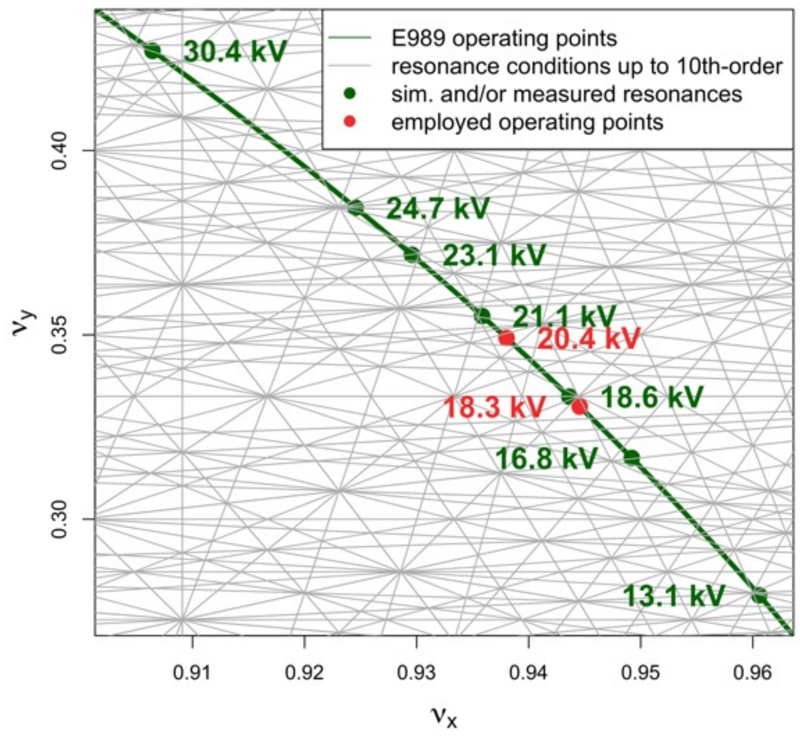

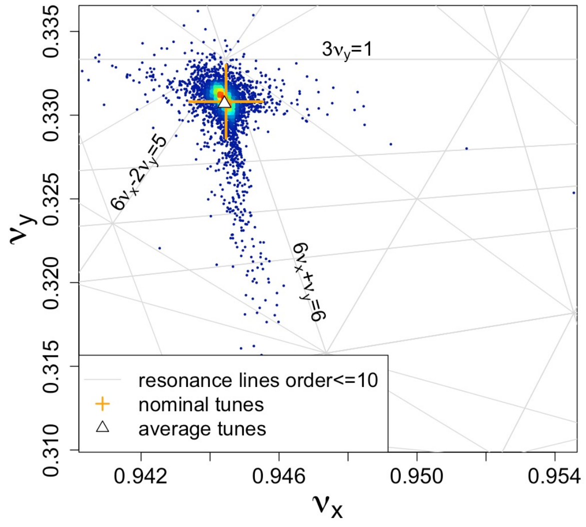

- Geometry of plates introduces nonlinearities.

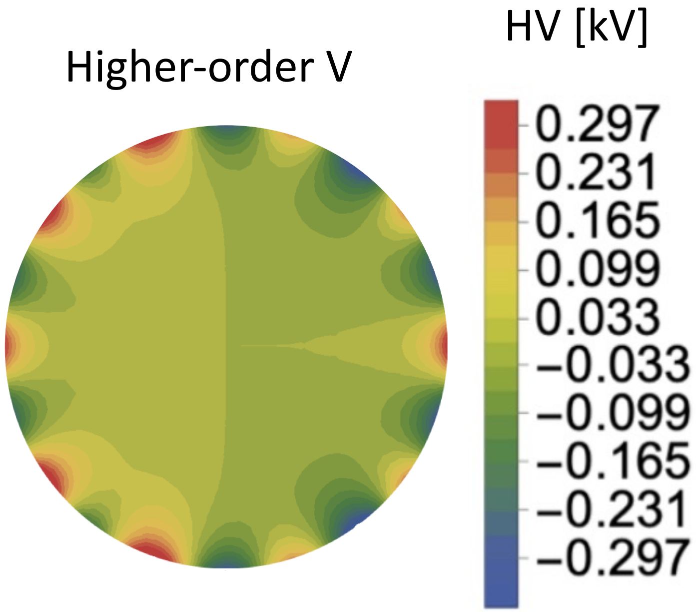

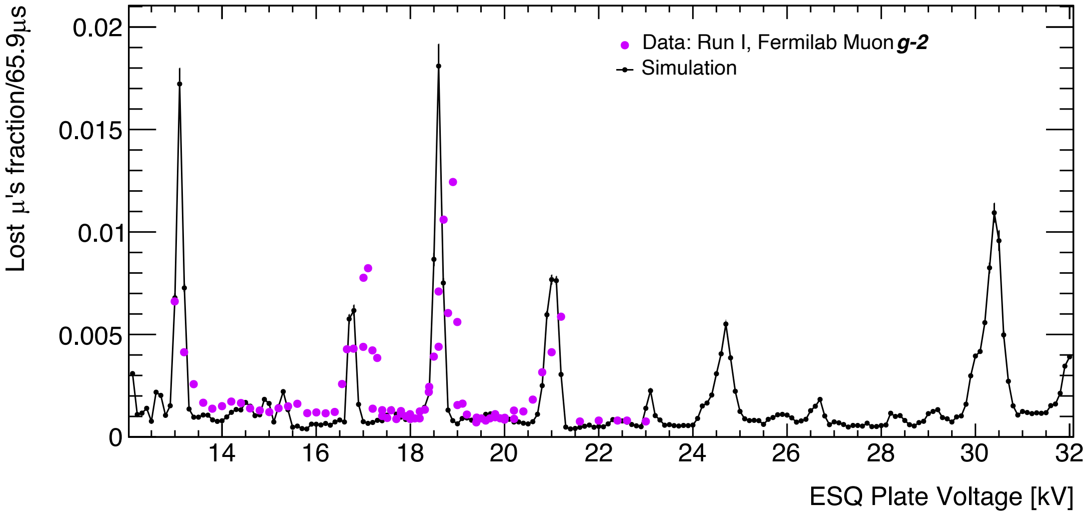

- $3Q_y = 1$ resonance near operation setpoint. Main driving term from magnetic skew sextupole.
- Beam decoherence ($\tau \approx 190\ \mu\text{s}$) driven by electric 20-pole.

Beam dynamics systematic effects

Nonnegligible when:

- Muon collimation changes overall phase (C_{ml}). [-11(5) ppb]
- Muon beam drifts during measurement (C_{pa}). [-158(75) ppb]
- Momentum-dependent beam decay changes phase (C_{dd}).

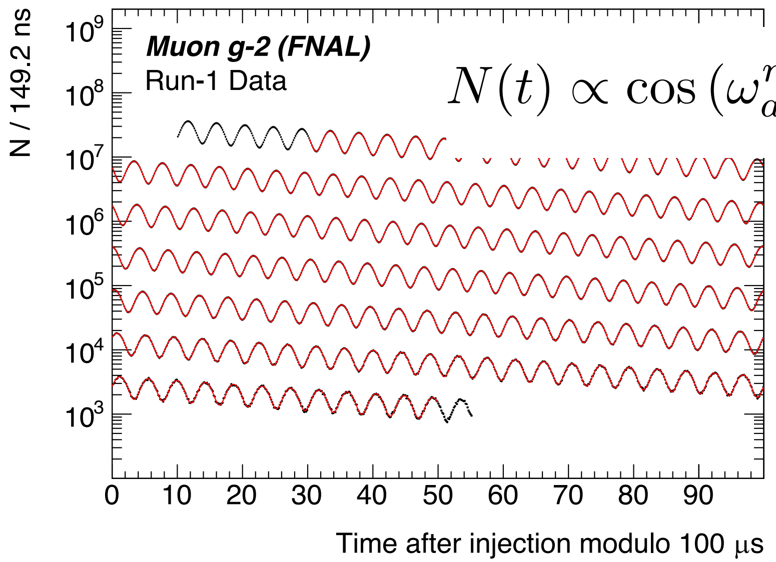

$$N(t) \propto \cos\left(\omega_a^m t + \varphi_0(t)\right) = \cos\left(\omega_a\left[1 + \left\langle\frac{\Delta\omega_a}{\omega_a}\right\rangle + \frac{1}{\omega_a}\frac{d\varphi_0}{dt}\right] t + \varphi_0 + \cdots\right)$$

$$\frac{d\mathbf{S}}{dt} = \boldsymbol{\omega}_s \times \mathbf{S}\,, \quad \boldsymbol{\omega}_s = -\frac{q}{m}\left[\left(a + \frac{1}{\gamma}\right)\mathbf{B} - a\frac{\gamma}{\gamma+1}(\boldsymbol{\beta}\cdot\mathbf{B})\boldsymbol{\beta} - \left(a + \frac{1}{\gamma+1}\right)\frac{\boldsymbol{\beta}\times\mathbf{E}}{c}\right]$$

Nonnegligible when:

- Muon beam has nonzero momentum spread (C_e). [489(53) ppb]
- Muons exhibit vertical oscillations (C_p). [180(13) ppb]

$$\omega_a = \omega_a^m\left[1 + C_e + C_p + C_{ml} + C_{dd} + C_{pa}\right]$$

E-field correction

Pitch correction

Muon loss correction

Differential decay correction

Phase-Acceptance correction

*In red, Run-1 values.

Beam dynamics systematic effects: E-field correction

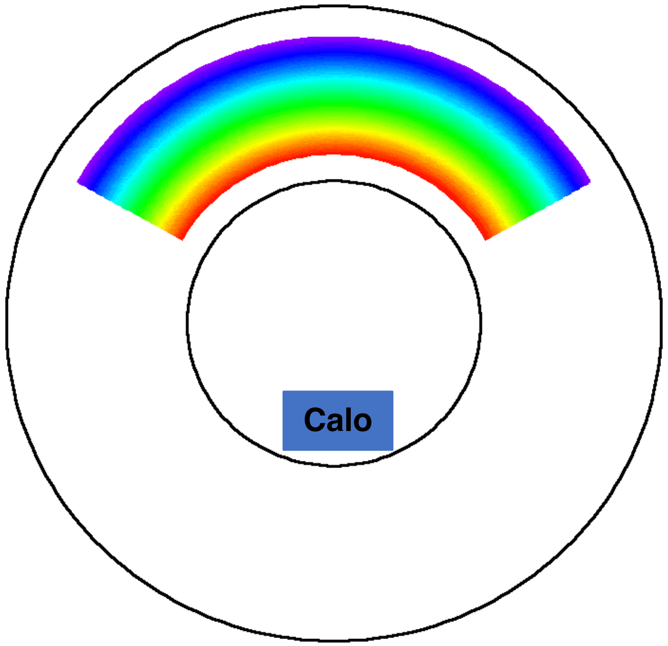

Higher Mom (Lower Freq)

Lower Mom (High Freq)

$$C_E = -\frac{n\beta^2}{1-n} 2\langle\delta^2\rangle \approx -480\ \text{ppb}$$

- Fast signal of muons population seen by Muon *g-2* calorimeter system builds from cyclotron frequencies distribution.

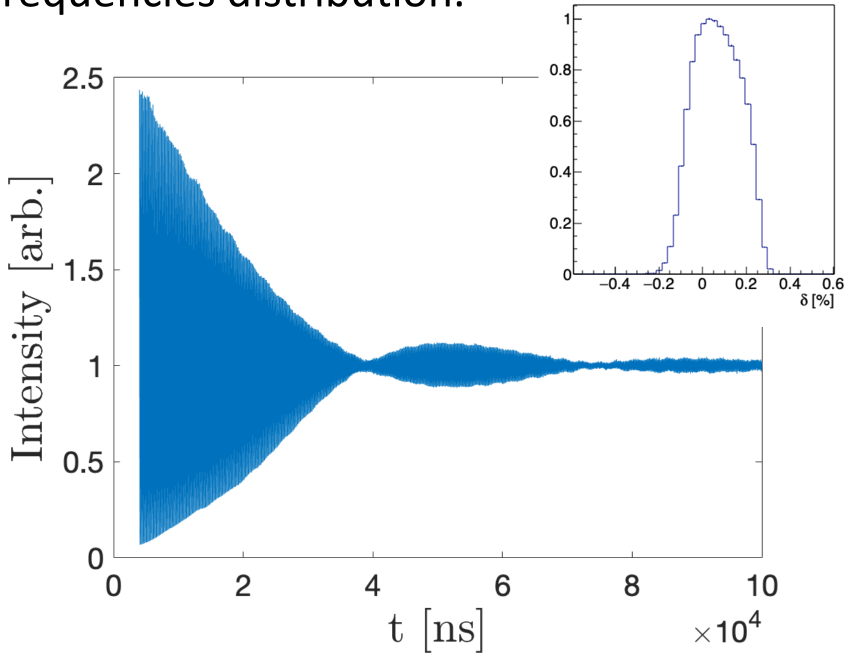

- Beam's momentum spread is measured from cyclotron frequencies distribution.

$$\frac{\Delta p}{p_0} = (1-n)\left(1 - \frac{f}{f_0}\right)$$

- Systematic error dominated by correlation between momentum and time-of-flights (~50 ppb):

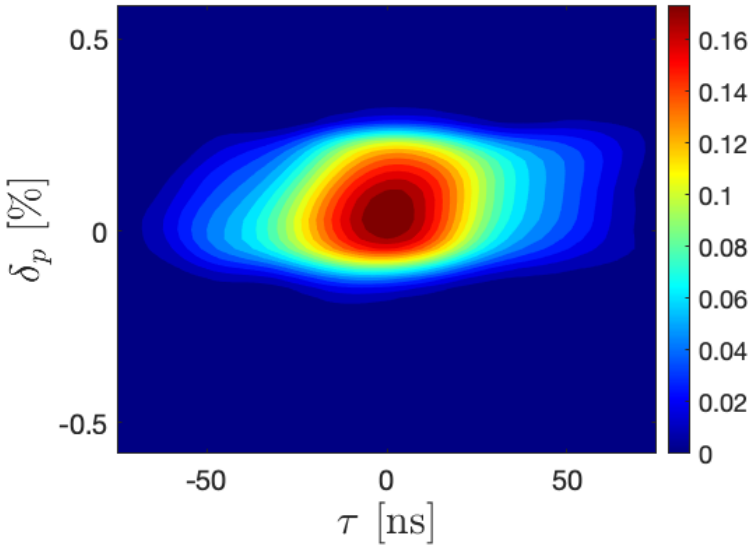

- With realistic tracking simulations, C_E standard expression is validated.

Beam dynamics systematic effects: Pitch correction

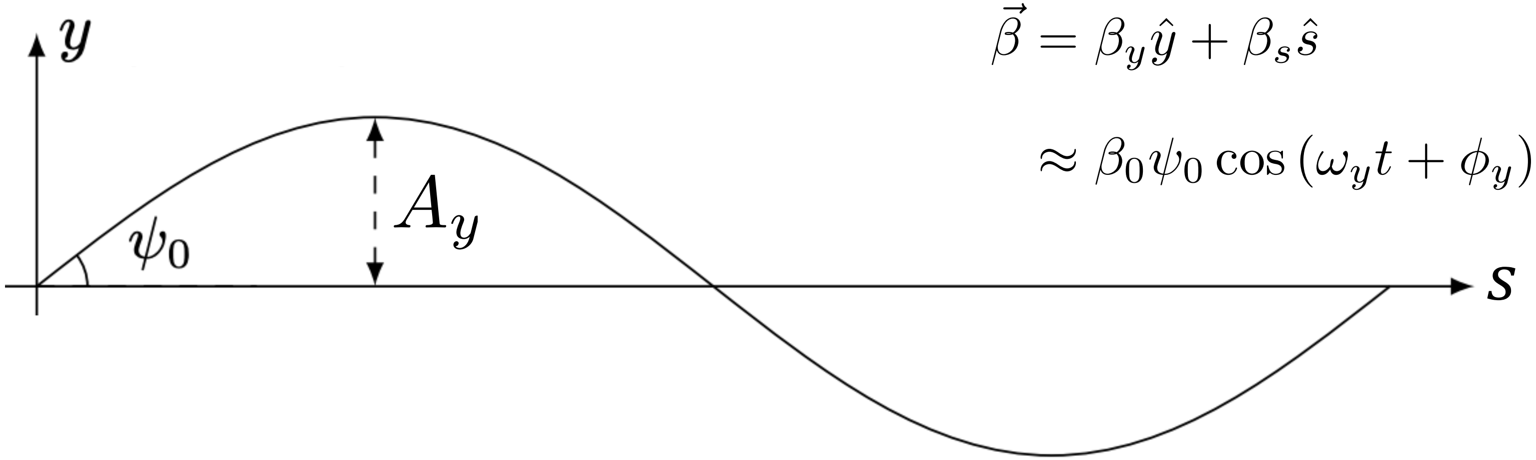

$$\vec{\beta} = \beta_y \hat{y} + \beta_s \hat{s}$$

$$\approx \beta_0 \psi_0 \cos\left(\omega_y t + \phi_y\right) \hat{y} + \beta_0 \left(1 - \frac{\psi_0^2}{2} \cos^2\left(\omega_y t + \phi_y\right)\right) \hat{s}$$

$\omega_a \approx 1.44$ rad/µs, $\omega_y \approx 13.8$ rad/µs

$$C_p = \left\langle \frac{\psi_0^2}{4} \left(1 + \frac{\omega_a^2}{\gamma_0^2 \left(\omega_y^2 - \omega_a^2\right)}\right) \right\rangle$$

$$\approx \frac{\langle \psi_0^2 \rangle}{4} = \frac{\langle y'^2 \rangle}{2} \approx \frac{n}{2\rho_0^2} \langle y^2 \rangle = \frac{n}{4\rho_0^2} \langle A_y^2 \rangle$$

$C_p = 180$ ppb, $\delta C_p = 13$ ppb for Run-1

Vertical position

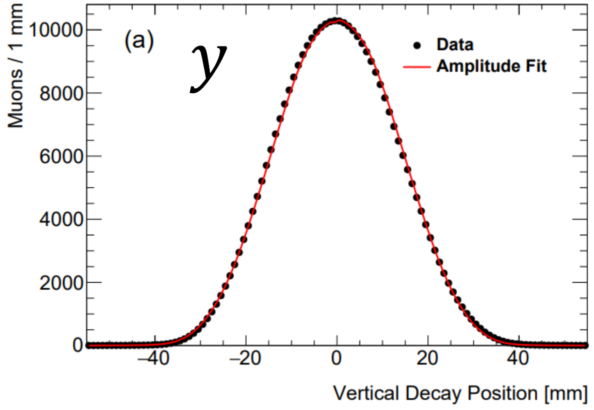

Betatron amplitude

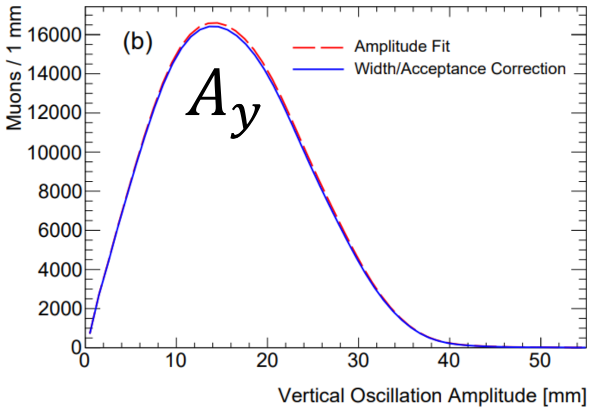

- Systematic errors dominated by tracking reconstruction and quadrupole calibration.

Beam dynamics systematic effects: Muon loss correction

- Bias from phase-momentum correlation and momentum-dependent muon loss:

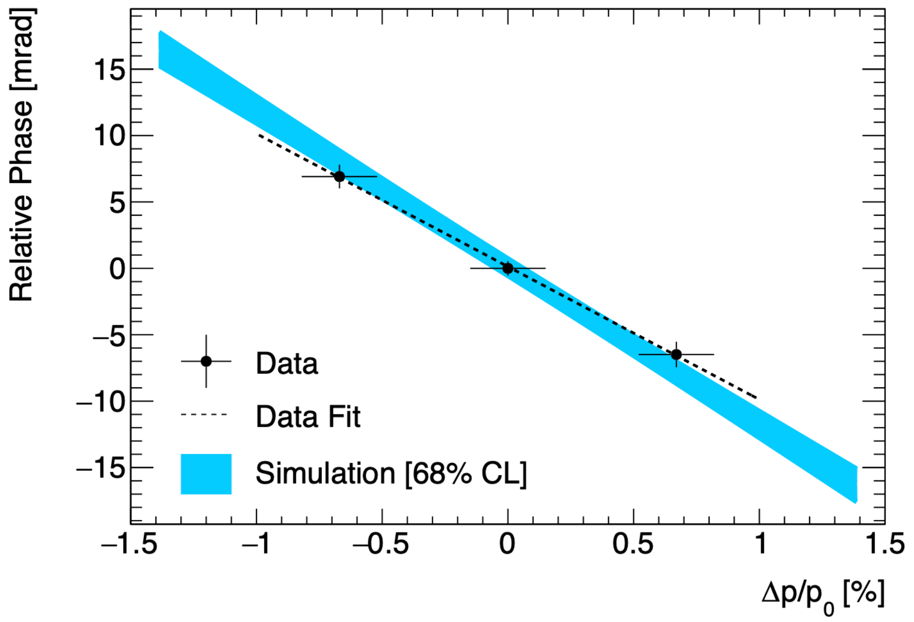

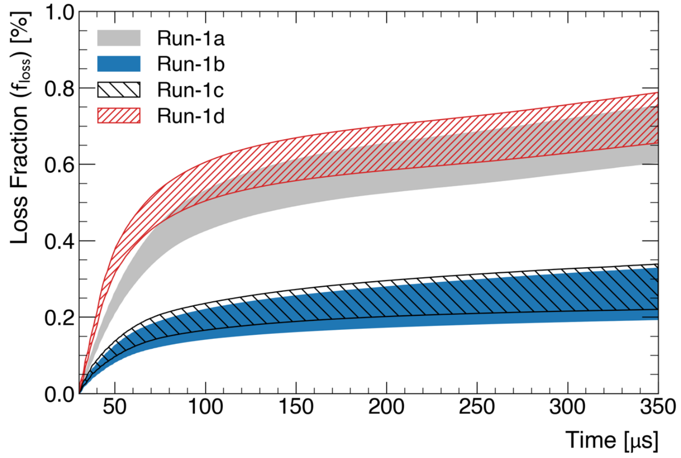

$$\frac{d\varphi_0}{dt} = \frac{d\varphi_0}{d\langle p\rangle}\frac{d\langle p\rangle}{dt}$$

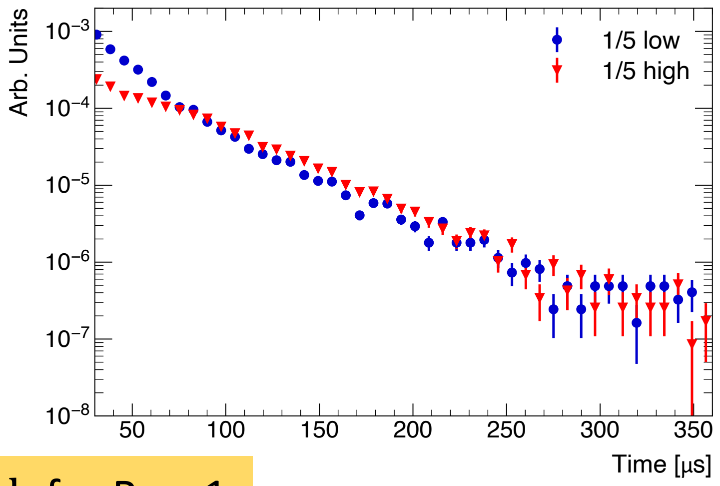

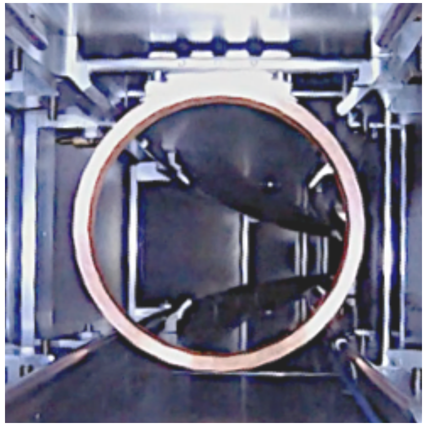

- Muon loss greatly reduced in posterior Runs.
- Differential decay correction follows same principles.

$C_{ml} = -11(5)$ ppb for Run-1

Beam dynamics systematic effects: Phase-Acceptance correction

- Unstable transverse motion of muon beam, detection acceptance, and spatial dependence of phase bias ω_a:

$$\varphi_0^{c_k}(t) = \arctan \frac{\sum_{ij} M_{T,k}(x_i, y_j, t) \cdot \varepsilon_{c,k}(x_i, y_j) \cdot A_k(x_i, y_j) \cdot \sin(\varphi_{0,k}(x_i, y_j))}{\sum_{ij} M_{T,k}(x_i, y_j, t) \cdot \varepsilon_{c,k}(x_i, y_j) \cdot A_k(x_i, y_j) \cdot \cos(\varphi_{0,k}(x_i, y_j))}$$

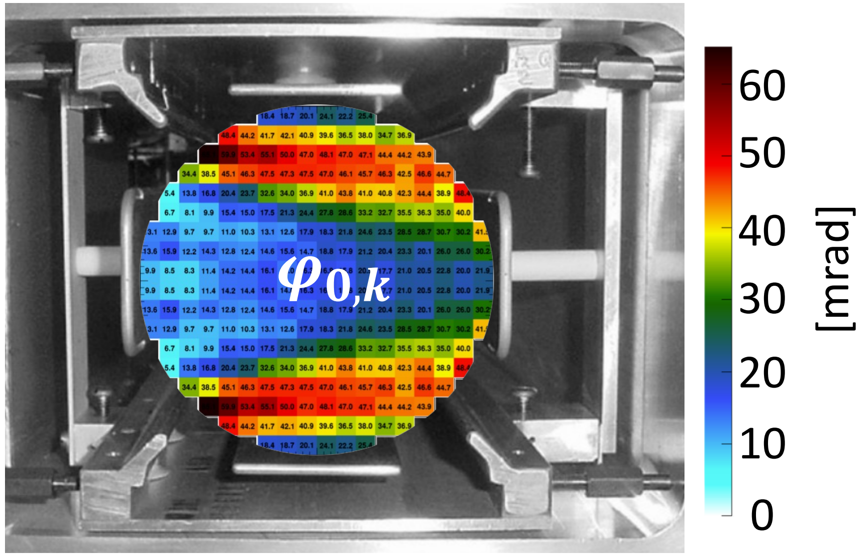

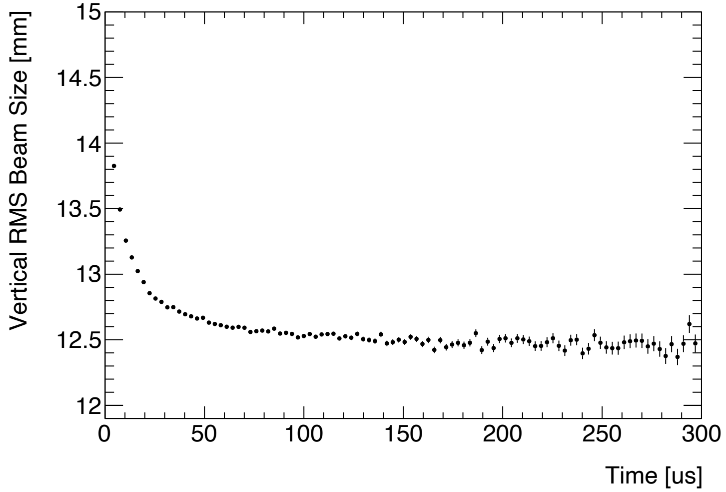

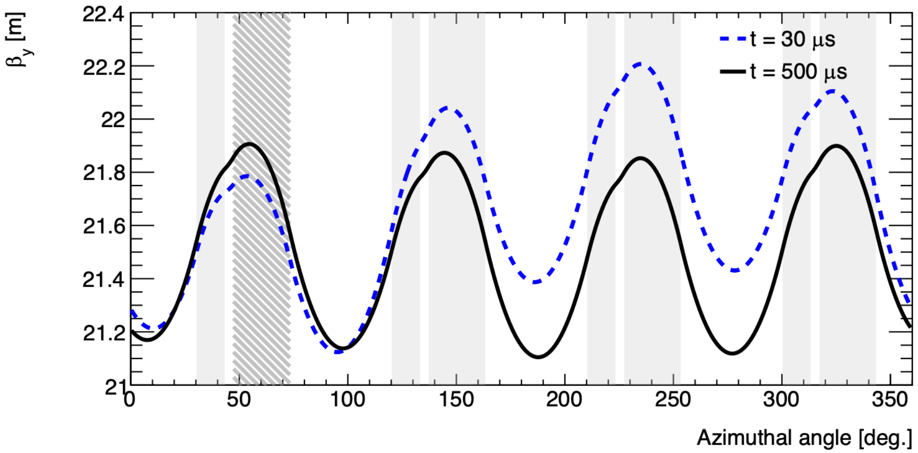

$C_{pa} = -158(75)$ ppb for Run-1

Beam dynamics systematic effects: ω_a and CBO

- Beam betatron motion and detector acceptance introduce additional oscillations in positron histogram.

Physical frequency	Calculated expression	Frequency (rad/μs) $n = 0.108$	Frequency (rad/μs) $n = 0.120$
ω_c	v/R_0	42.15	42.15
ω_x	$\sqrt{1-n}\omega_c$	39.81	39.54
ω_y	$\sqrt{n}\omega_c$	13.85	14.60
ω_{CBO}	$\omega_c - \omega_x$	2.34	2.61
ω_{VW}	$\omega_c - 2\omega_y$	14.45	12.95
ω_a	$e a_\mu B/m$	1.44	1.44

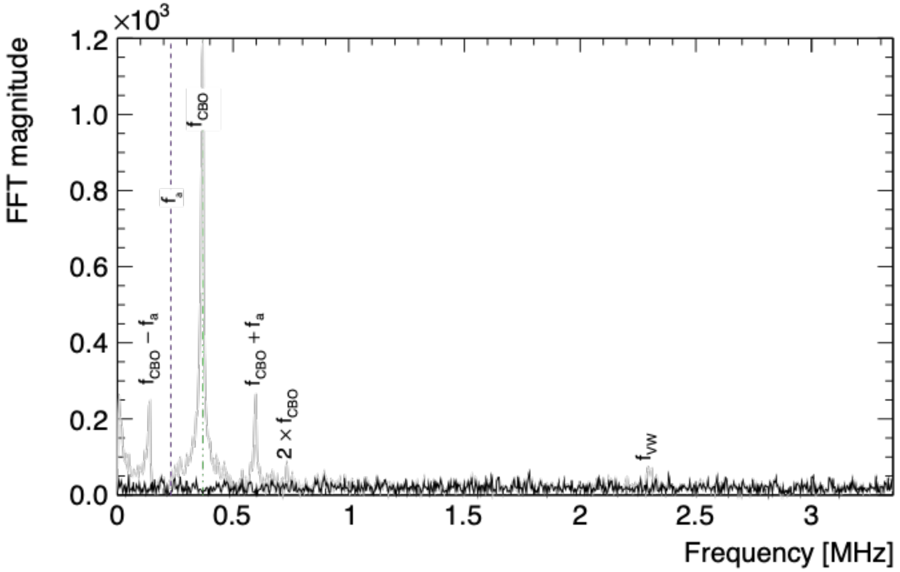

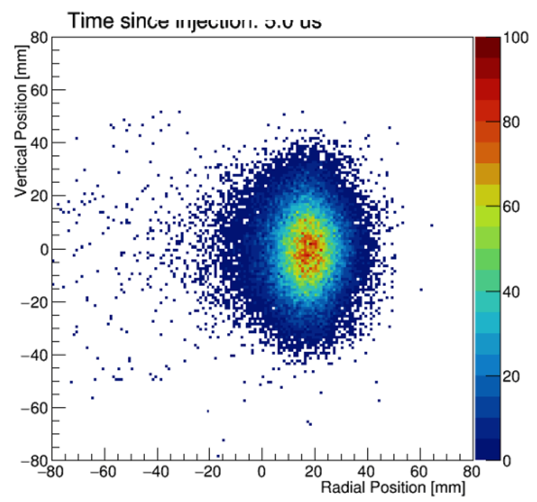

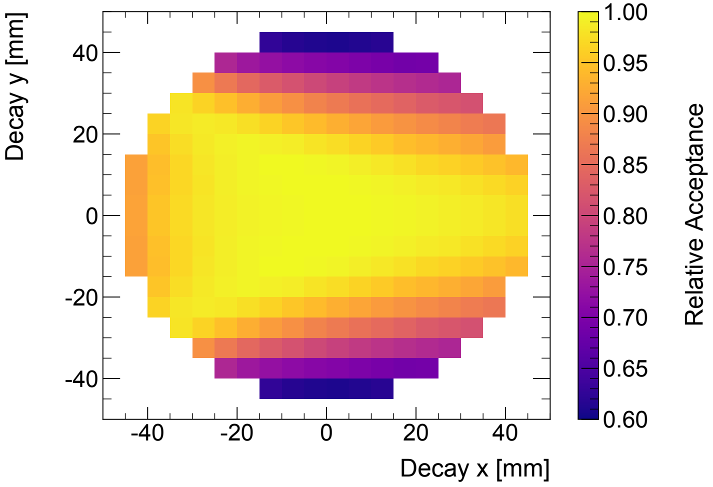

$$F(t) = N_0 \cdot N_x(t) \cdot N_y(t) \cdot \Lambda(t) \cdot e^{-t/\gamma\tau_\mu} \times \left[1 + A_0 \cdot A_x(t) \cdot \cos\left(\omega_a(R)t + \phi_0 \cdot \phi_x(t)\right)\right]$$

$$N_x(t) = 1 + e^{-1t/\tau_{\mathrm{CBO}}} A_{N,x,1,1} \cos(1\omega_{\mathrm{CBO}} t + \phi_{N,x,1,1}) + e^{-2t/\tau_{\mathrm{CBO}}} A_{N,x,2,2} \cos(2\omega_{\mathrm{CBO}} t + \phi_{N,x,2,2}),$$

$$N_y(t) = 1 + e^{-1t/\tau_y} A_{N,y,1,1} \cos(1\omega_y t + \phi_{N,y,1,1}) + e^{-2t/\tau_y} A_{N,y,2,2} \cos(1\omega_{\mathrm{VW}} t + \phi_{N,y,2,2}),$$

$$A_x(t) = 1 + e^{-1t/\tau_{\mathrm{CBO}}} A_{A,x,1,1} \cos(1\omega_{\mathrm{CBO}} t + \phi_{A,x,1,1}),$$

$$\phi_x(t) = 1 + e^{-1t/\tau_{\mathrm{CBO}}} A_{\phi,x,1,1} \cos(1\omega_{\mathrm{CBO}} t + \phi_{\phi,x,1,1}).$$

Summary, current status and plans

$$\frac{\omega_a}{\tilde{\omega}'_p(T_r)} = \frac{f_{\text{clock}}\, \omega_a^m \,(1 + C_e + C_p + C_{ml} + C_{pa})}{f_{\text{calib}}\, \langle \omega_p(x,y,\phi) \times M(x,y,\phi) \rangle \,(1 + B_k + B_q)}$$

- We are smoothly running Run-5
- Target statistic expected to be reached in 2022-2023.
- New scraping mode currently being tested.
- ESQ system stable after Run-1, as well as magnet temperature. Better beam injection.
- Analysis and further measurements expected to reduce systematic uncertainties.

PHYSICAL REVIEW LETTERS **126,** 141801 (2021)

TABLE II. Values and uncertainties of the $\mathcal{R}'_\mu$ correction terms in Eq. (4), and uncertainties due to the constants in Eq. (2) for a_μ. Positive C_i increase a_μ and positive B_i decrease a_μ.

Quantity	Correction terms (ppb)	Uncertainty (ppb)
ω_a^m (statistical)	···	434
ω_a^m (systematic)	···	56
C_e	489	53
C_p	180	13
C_{ml}	−11	5
C_{pa}	−158	75
$f_{\text{calib}} \langle \omega_p(x,y,\phi) \times M(x,y,\phi) \rangle$	···	56
B_k	−27	37
B_q	−17	92
$\mu'_p(34.7°)/\mu_e$	···	10
m_μ/m_e	···	22
$g_e/2$	···	0
Total systematic	···	157
Total fundamental factors	···	25
Totals	544	462

*From Run-1 analysis

THANKS!

BACKUP

Run-1 Results

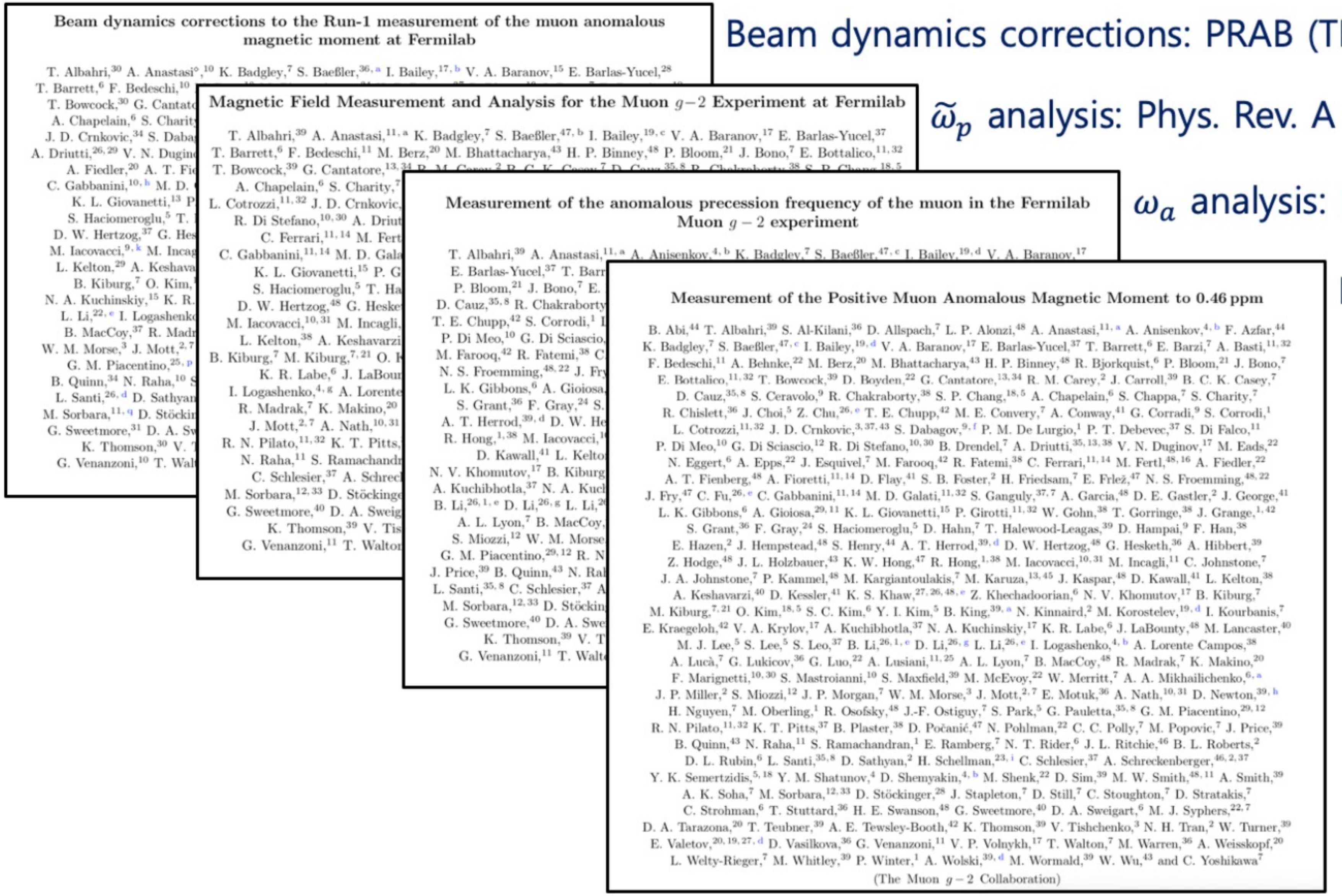

Beam dynamics corrections: PRAB (TBD) arXiv:2104.03240

$\tilde{\omega}_p$ analysis: Phys. Rev. A **103**, 042208

ω_a analysis: Phys. Rev. D **103**, 072002

Phys. Rev. Lett. **126**, 141801

Current status and future

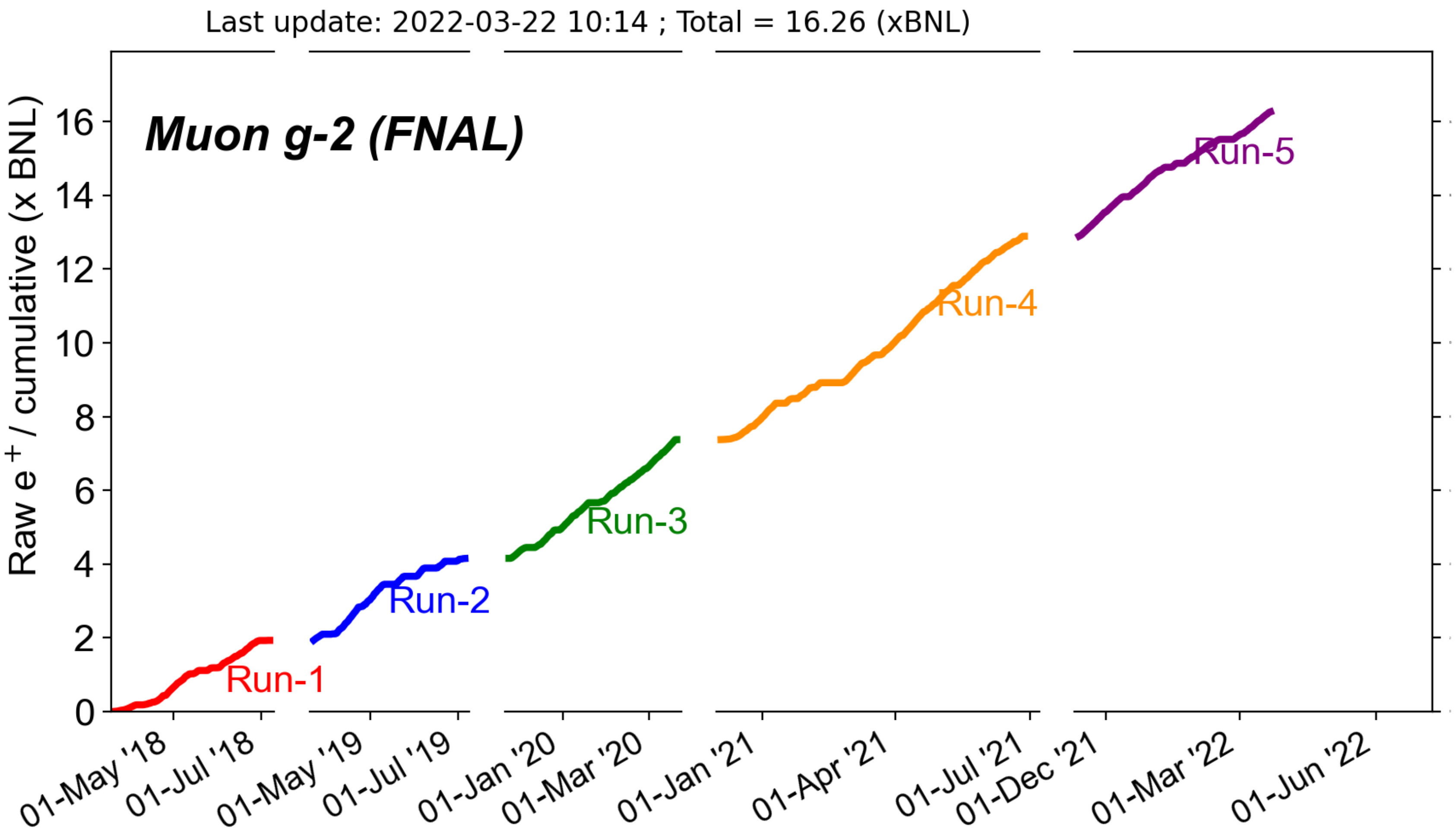

Remarks

- Latest experimental result of the muon anomaly (measured to 460 ppb precision) has been released.
- The new experimental average increased the tension with the Standard Model to 4.2σ.
- Run-2/3 analysis is ongoing which will improve the sensitivity by a factor of 2.
- E989 is now in the middle of Run-5, approaching the target statistics. Further results coming soon!